Available online at www.sciencedirect.com
SCIENCE DIRECT
Palaeoworld
Palaeoworld 15 (2006) 3–30
www.elsevier.com/locate/palwor

Research paper

End-Permian mass extinction pattern in the northern peri-Gondwanan region

Shu Zhong Shen [a,*], Chang-Qun Cao [a], Charles M. Henderson [b], Xiang-Dong Wang [a], Guang R. Shi [c], Yue Wang [a], Wei Wang [a]

[a] *State Key Laboratory of Palaeobiology and Stratigraphy, Nanjing Institute of Geology and Palaeontology, Chinese Academy of Sciences, 39 East Beijing Road, Nanjing, Jiangsu 210008, PR China*
[b] *Department of Geology and Geophysics, University of Calgary, Calgary, Alberta, Canada T2N 1N4*
[c] *School of Ecology and Environment, Deakin University, Melbourne Campus, 221 Burwood Highway, Burwood, Vic. 3125, Australia*

Received 1 July 2005; received in revised form 8 March 2006; accepted 31 March 2006

Abstract

The Permian-Triassic extinction pattern in the peri-Gondwanan region is documented biostratigraphically, geochemically and sedimentologically based on three marine sequences deposited in southern Tibet and comparisons with the sections in the Salt Range, Pakistan and Kashmir. Results of biostratigraphical ranges for the marine faunas reveal an end-Permian event comparable in timing with that known at the Meishan section in low palaeolatitude as well as Spitsbergen and East Greenland in northern Boreal settings although biotic patterns earlier in the Permian vary. The previously interpreted delayed extinction (Late Griesbachian) at the Selong Xishan section is not supported by our analysis. The end-Permian event exhibits an abrupt marine faunal shift slightly beneath the Permian-Triassic boundary (PTB) from benthic taxa- to nektic taxa-dominated communities. The climate along the continental margin of Neo-Tethys was cold before the extinction event. However, a rapid climatic warming event as indicated by the southward invasion of abundant warm-water conodonts, warm-water brachiopods, calcareous sponges, and gastropods was associated with the extinction event. Stable isotopic values of $\delta^{13}C_{carb}$, $\delta^{13}C_{org}$ and $\delta^{18}O$ show a sharp negative drop slightly before and during the extinction interval. Sedimentological and microstratigraphical analysis reveals a Late Permian regression, as marked by a Caliche Bed at the Selong Xishan section and the micaceous siltstone in the topmost part of the Qubuerga Formation at the Qubu and Tulong sections. The regression was immediately followed by a rapid transgression beneath the PTB. The basal Triassic rocks fine upward, and are dominated by dolomitic packstone/wackestone containing pyritic cubes, bioturbation and numerous tiny foraminifers, suggesting that the studied sections were deposited during the initial stage of the transgression and hence may not have been deeply affected by the anoxic event that is widely believed to characterise the zenith of the transgression.

Keywords: End-Permian; Mass extinction; Peri-Gondwanan region; Climatic warming; Sea-level changes

1. Introduction

The end-Permian mass extinction is the most severe in the geologic record (Raup, 1979; Sepkoski, 1984; Erwin, 1993; Hallam and Wignall, 1997). Previous research has suggested a very abrupt extinction event among marine and terrestrial organisms (Rampino and Adler, 1998; Bowring et al., 1998; Jin et al., 2000; Twitchett et al., 2001, 2004; Smith and Ward, 2001; Erwin et al., 2002; Shen and Shi, 2002). Recent popular mechanisms for the mass extinction include: bolide impact (Becker et al., 2001, 2004), volcanism related to the Siberian

* Corresponding author. Tel.: +86 25 3282131; fax: +86 25 3282131.
E-mail address: szshen@nigpas.ac.cn (S.Z. Shen).

1871-174X/$ – see front matter
doi:10.1016/j.palwor.2006.03.005

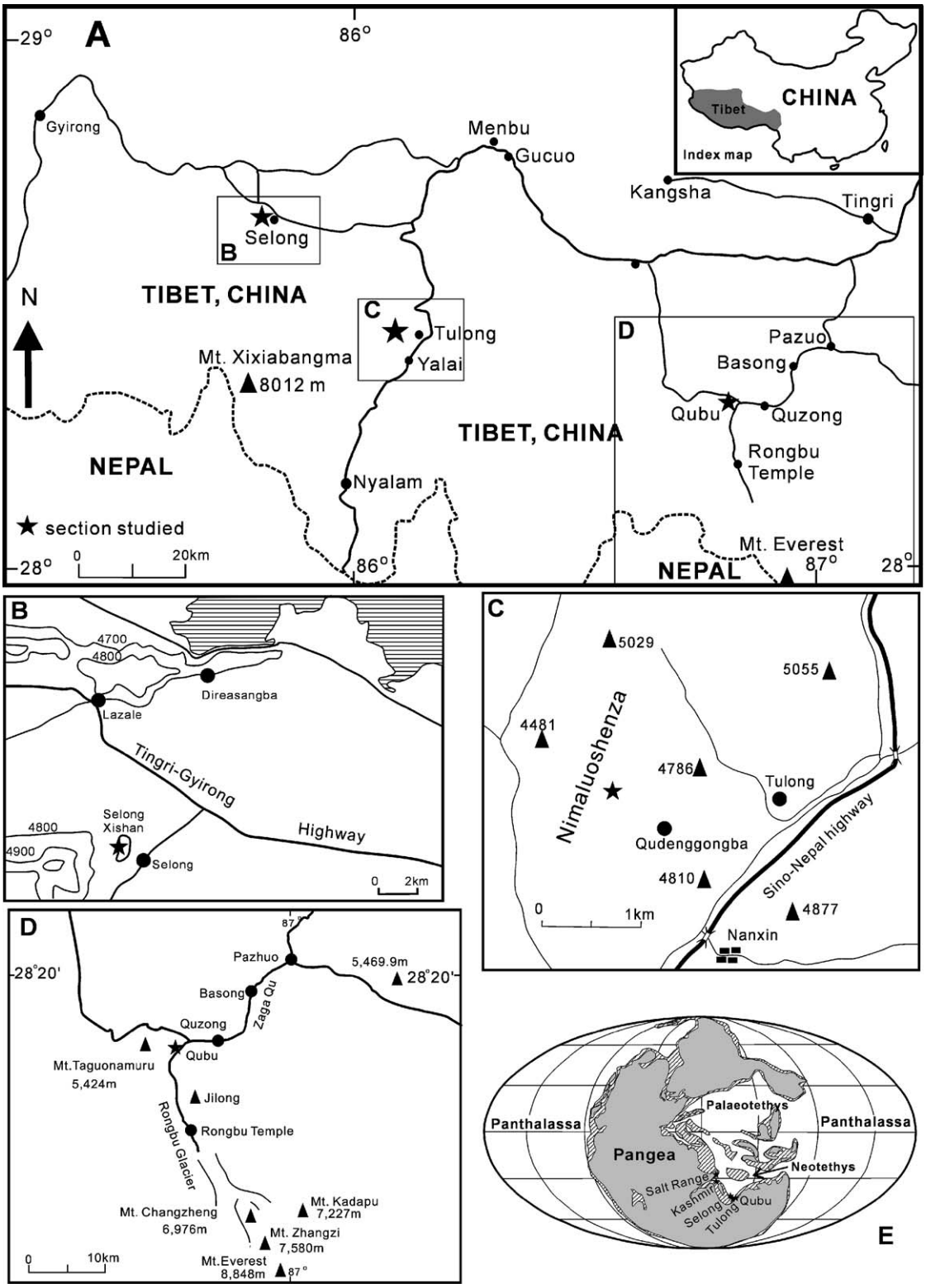

Fig. 1. Locality map showing the location of the studied sections. (A) Map showing the studied area in southern Tibet. (B) Detailed map showing the location of the Selong Xishan section. (C) Detailed map showing the location of the Tulong section. (D) Detailed map showing the location of the Qubu section. (E) Reconstruction map showing the palaeoposition of the sections during the P–T transition (base map after Ziegler et al., 1997).

Trap (Renne et al., 1995; Bowring et al., 1998), and global anoxia associated with sea-level rise (Wignall and Hallam, 1992; Hallam and Wignall, 1997; Isozaki, 1997). Information on the timing, magnitude and nature of the event has come mostly from low and middle palaeolatitude sites in and around the Palaeo-Tethys (Wignall and Hallam, 1992; Bowring et al., 1998; Jin et al., 2000; Kaiho et al., 2001; Krull et al., 2004; Mundil et al., 2001, 2004), Panthalassa from Japan (Isozaki, 1997) and northern temperate and Arctic sites (Henderson, 1997; Henderson and Baud, 1997; Wang et al., 1994; Wignall et al., 1998; Wignall and Newton, 2003; Twitchett et al., 2001). The Permian-Triassic boundary succession in southern higher palaeolatitude settings has also been a region for major research on the PTB (e.g. Wignall and Hallam, 1993; Jin et al., 1996; Morante, 1996; Shen and Jin, 1999) and has recently become a focus of research to unravel the latest Permian extinction pattern of marine and non-marine faunas (Smith and Ward, 2001; Shen and Cao, 2002; Brookfield et al., 2003; Krystyn et al., 2003; Sarkar et al., 2003; Retallack et al., 2003; Wignall and Newton, 2003; Twitchett et al., 2004). This paper con-

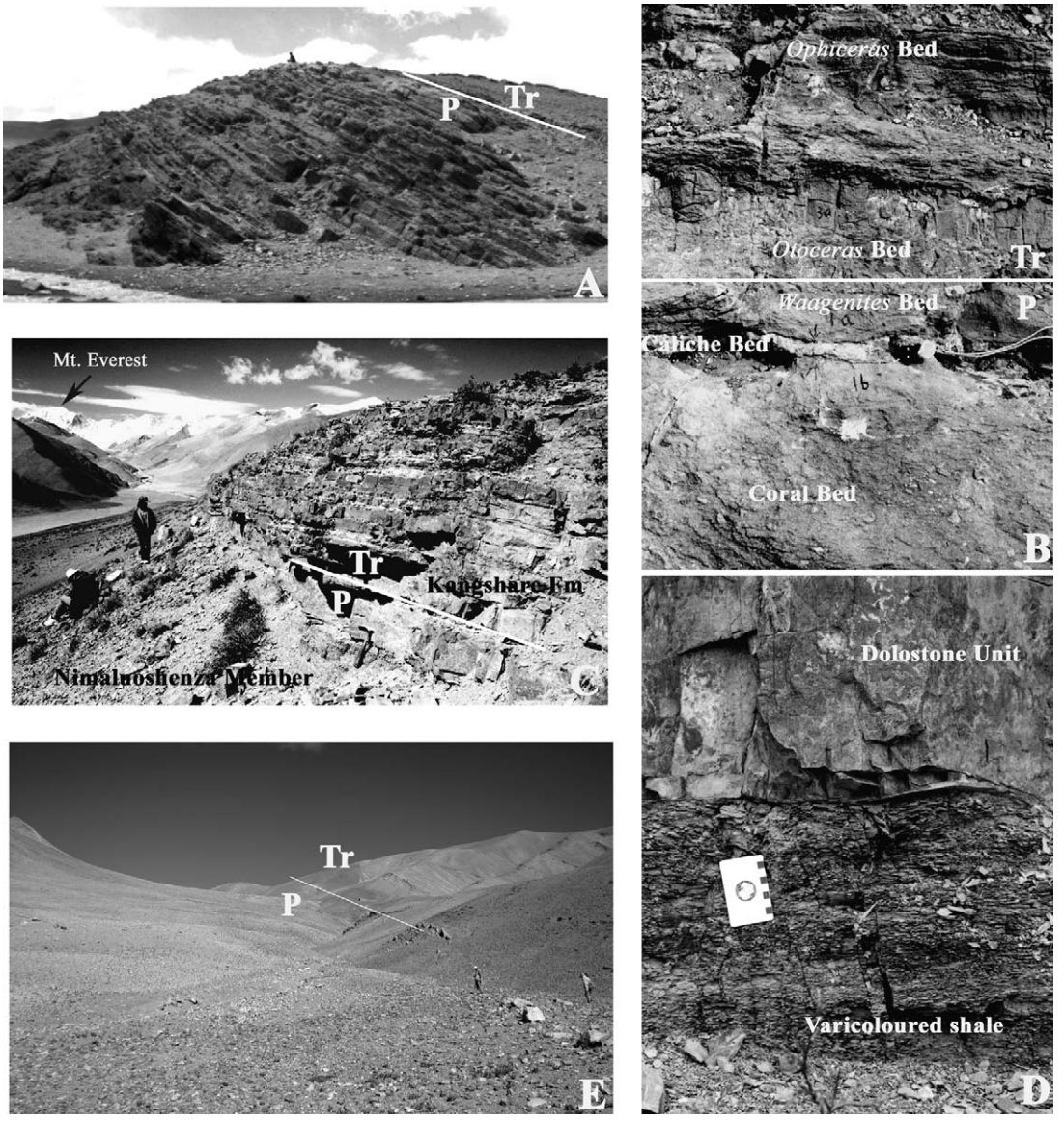

Fig. 2. Photos of the three sections in southern Tibet. (A) Selong Xishan section. (B) PTB beds at the Selong Xishan section. (C) PTB beds at the Qubu section. (D) Close view of the contact between the Qubuerga Formation and the Tulong Formation at the Qubu section. (E) Distal view of the Tulong section.

tributes considerable new and newly interpreted data that have significant bearing on PTB interval interpretations for the region.

The peri-Gondwanan region straddles the northern margin of Gondwana and the southern margin of the Palaeo-Tethys/Neo-Tethys. Three key areas have been chosen as the focus of the present study: southern Tibet, Kashmir, and the Salt Range of Pakistan (Fig. 1E). Palaeogeographically, this region was located within the temperate mesothermal zone. Palaeobiogeographically during the Permian, the region has been classified as representing a transitional biogeographical zone between the palaeoequatorial Cathaysian Province and the temperate/polar provinces of the Gondwanan Realm (Shi et al., 1995) or the peri-Gondwana Cool Water Province of Mei and Henderson (2001).

Despite its critical palaeogeographical and palaeobiogeographical settings during the Permian-Triassic transition, our understanding of the peri-Gondwanan region in connection to the end-Permian mass extinction remains equivocal. In part, this uncertainty can be attributed to the longstanding misunderstanding with regard to the age of the Late Permian deposits in this region. Prior to the 1990s, many workers considered that there was a major Late Permian hiatus across the peri-Gondwanan region (e.g. Grant, 1970; Wang et al., 1989; Xia and Zhang, 1992; Wang and Wang, 1995). However, more recent biostratigraphical, sedimentological and geochemical studies, particularly those from southern Tibet (e.g. Jin et al., 1996; Shen et al., 2003a; Wignall and Newton, 2003), demonstrate in fact that the Late Permian succession in southern Tibet is continuous across the Permian-Triassic transitional interval and bears no evidence for hiatus. This conclusion is significant because it means that these higher palaeo-latitude peri-Gondwanan PTB sections may be used to investigate the nature of the marine faunal shift across the PTB in southern higher palaeolatitude settings (Fig. 1E).

In this paper we present: (1) additional data and new interpretations from previous studies of the Selong Xishan section in southern Tibet; (2) end-Permian extinction patterns of two new marine PTB sections in southern Tibet (Figs. 1 and 2); and (3) a comparison with other peri-Gondwanan sections in Kashmir and the Salt Range, Pakistan (Fig. 1E) in view of end-Permian mass extinction patterns. The focus of the paper is on palaeontological, sedimentological, stratigraphical and isotope geochemical characteristics of the PTB sections, although brief discussions on the cause of the recognised patterns are provided where appropriate. It is hoped that our study can serve as a starting point for further synthesis and elucidation of higher latitude end-Permian mass extinction events and processes that will provide a contrast to equatorial signatures.

2. Selong Xishan section

The Selong Xishan section is situated about 1 km northwest of Selong in Nyalam County and about 700 km southwest of Lhasa, Tibet, China (Figs. 1A,B and 2A,B). Extensive biostratigraphical studies have been conducted at the section (Wang et al., 1989; Xia and Zhang, 1992; Orchard et al., 1994; Mei, 1996; Shi and Shen, 1997; Shen and Jin, 1999; Shen et al., 2000, 2001). A general study regarding the biostratigraphy, sedimentology, and geochemistry of this section was presented by Jin et al. (1996). Recently, Wignall and Newton (2003), based mainly on small foraminifers and calcareous sponges from this section, claimed a late Griesbachian mass extinction, which is about half a million years later than that at the Meishan section of South China in the Palaeoequatorial setting. However, as will be described in detail below, the results of our study, based on the most abundant brachiopods and other benthic fossils, are different from their conclusions; Retallack (2004) also questioned this diachroneity.

2.1. Faunal shift

The Selong Group and the overlying *Waagenites* Bed of the basal Kangshare Formation contain 49 Late Permian brachiopod species associated with corals, bryozoans and numerous crinoids (Fig. 3). These brachiopod species have been systematically described by Shi and Shen (1997), Shen and Jin (1999) and Shen et al. (2000, 2001). A composite range chart of brachiopods, corals, conodonts, foraminifers and ammonoids indicates that the major faunal extinction is within the *Waagenites* Bed just below the PTB (Fig. 4). Among the 49 brachiopod species, 12 species, mostly ranging from the underlying Selong Group, disappeared at the PTB and six species disappeared at the top of the Selong Group (Shen et al., 2000, 2001). None of the Permian brachiopods extends into the Induan (Fig. 4). Permian corals and some bryozoans also disappeared in the *Waagenites* Bed (Fig. 3L). In addition to the above-mentioned 12 species, 21 brachiopod species disappeared within the topmost 2.15 m of the Upper Permian Selong Group. It is thus clear that the stratigraphic distribution of the brachiopods at the Selong Xishan section exhibits a relatively rapid extinction pattern through the PTB interval (Fig. 4). As documented by many previous studies (e.g. Signor and Lipps, 1982; Marshall, 1995; Holland, 2000), the last projected occurrence may be higher than the

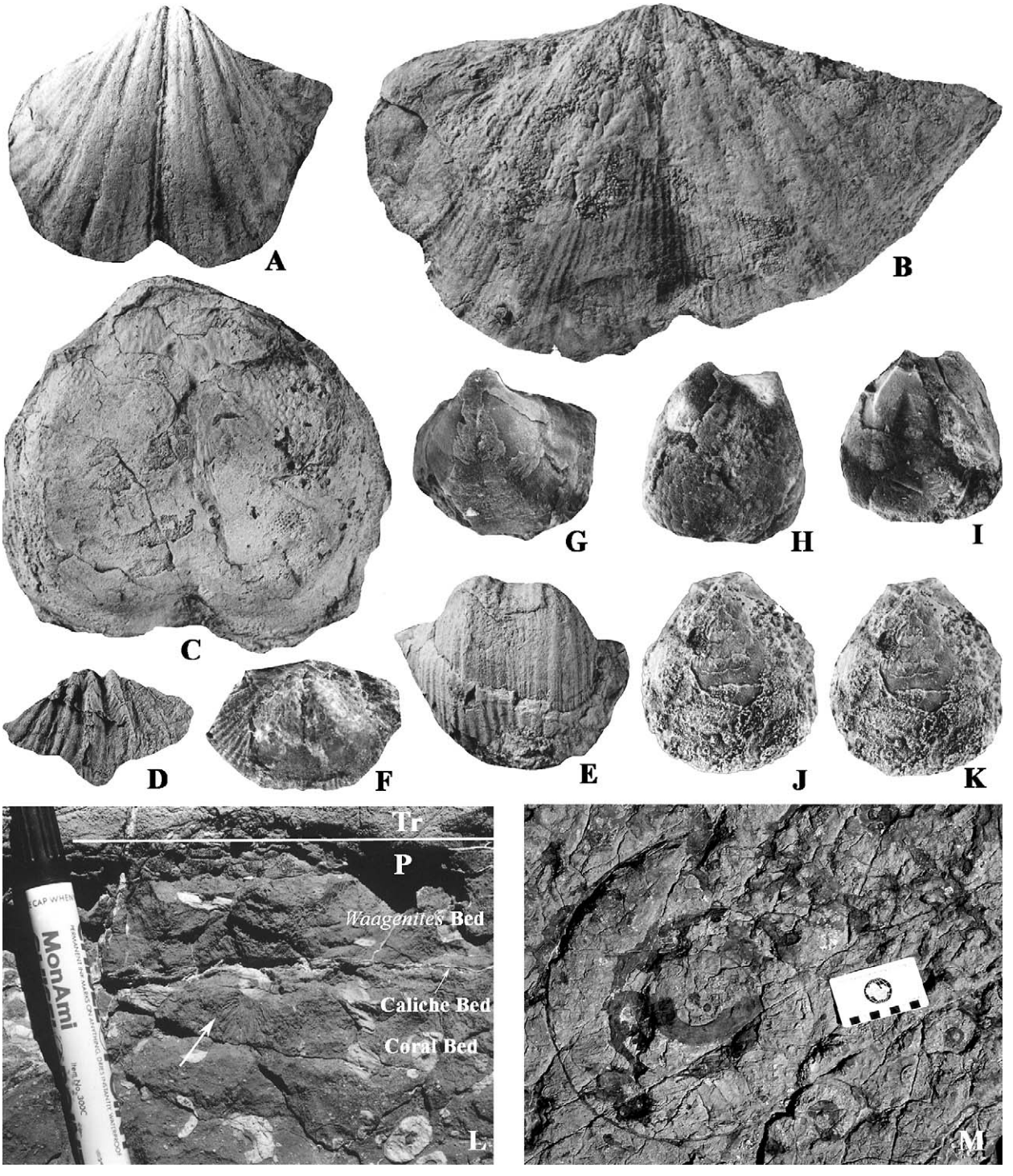

Fig. 3. Megafossils from the PTB beds at the Selong Xishan section. (A–E) Brachiopods with bipolar or Gondwana affinities from the Selong group: (A) *Spiriferella rajah*; (B) *Neospirifer* (*Neospirifer*) *kubeiensis*; (C) *Taeniothaerus densipustulatus*; (D) *Trigonotreta lightjacki*; (E) *Retimarginifera xizangensis*. (F–K) Brachiopods with cosmopolitan or Tethyan affinities from the *Waagenites* Bed of the basal Kangshare Formation; (F) *Tethyochonetes* sp., ×2; (G) *Martinia* sp., ×2; (H and I) *Martinia attenuatelloides*, ×2; (J and K) *Girtyella*? sp., ×2. (L) *Ufimia*? from the topmost part of the Coral Bed. M, Photo showing various ammonoids of different sizes in the lowest Triassic of the Selong Xishan section (scale bar in centimeter). All figures are natural sized unless otherwise indicated.

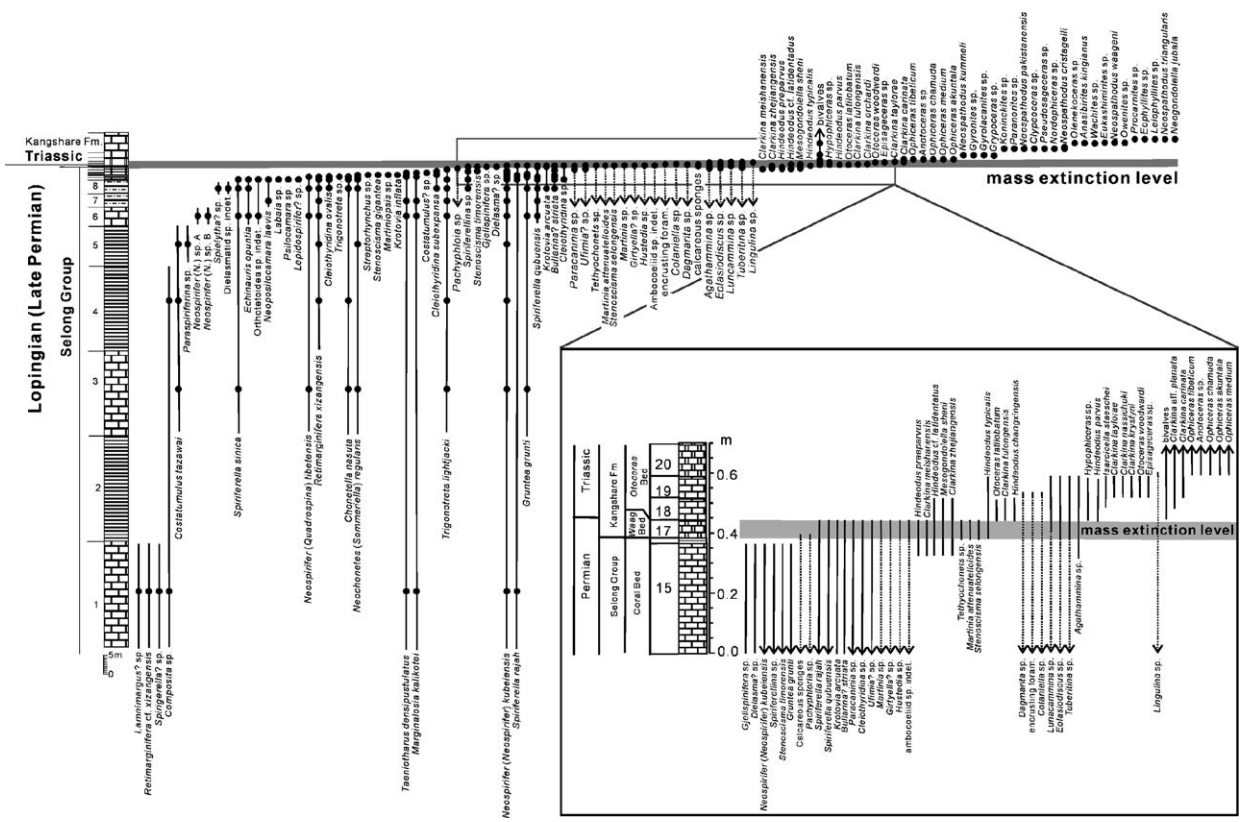

Fig. 4. Composite range chart of various fossil species at the Selong Xishan section. Permian-only species are arranged by last appearance and Triassic-only species are arranged by first appearance. Arrows indicate that taxa continue to be present in the underlying or overlying intervals. Solid lines indicate the presence of taxa at Selong, but dotted lines indicate that these taxa are found elsewhere at the same time. Data integrated from Wang et al. (1989); Xia and Zhang (1992); Orchard et al. (1994); Mei (1996); Shen and Jin (1999); Shen et al. (2000, 2001); Wignall and Newton (2003). Some conodonts are from newly processed samples.

actual stratigraphic record; therefore the actual extinction pattern may be even more rapid than that displayed, based on the actual last stratigraphic occurrence pattern. It may be argued that the Changhsingian strata at the Selong Xishan section are highly condensed and therefore may represent a long time. Clearly, the latest Changhsingian and the lower Induan strata are very condensed as several zones are represented by less than a metre of strata; pressure solution may have been enhanced along minor discontinuities that would be indicative of this condensation and thereby lead to the stylolitic nature of the *Waagenites* and *Otoceras* beds. However, the major extinction interval in the *Waagenites* Bed is well constrained by the conodont *Mesogondolella sheni* Zone associated with *Clarkina meishanensis* and *C. zhejiangensis* and the sharp drop of carbon isotopic

Fig. 5. Conodonts from the PTB beds at the Selong Xishan and Qubu sections. (A) *Mesogondolella sheni*, from the *Waagenites* Bed, Selong Xishan section; (B) *Mesogondolella sheni*, from Bed 18, Selong Xishan section; (C and D) *Clarkina zhejiangensis* (upper and oblique view, respectively), from Bed 18, Selong Xishan section; (E and F) *Mesogondolella sheni* (oblique and upper view, respectively), from top of Bed 15 (the Coral Bed), Selong Xishan section; (G) *Clarkina tulongensis*, from Bed 18, Selong Xishan section; (H and I) *Clarkina tulongensis* (upper and oblique view, respectively), from Bed 33, Qubu section; (J and K) *Mesogondolella sheni* (oblique and upper view, respectively), from top of Bed 15 (the Coral Bed), Selong Xishan section; (L and M) *Clarkina taylorae* (oblique and upper view, respectively), from Bed 33, Qubu section; (N and O) *Clarkina taylorae* (upper and oblique view, respectively), from Bed 19, Selong Xishan section; (P and Q) *Clarkina carinata* (oblique and upper view, respectively), from Bed 41, Qubu section; (R and S) *Clarkina zhejiangensis* (upper and oblique view, respectively), from top of Bed 15 (the Coral Bed), Selong Xishan section; (T and U) *Clarkina carinata* (oblique and upper view, respectively), from Bed 41, Qubu section; (V and W) *Clarkina tulongensis* (upper and oblique view, respectively), from Bed 33, Qubu section; (X and Y) *Clarkina krystyni* (upper and oblique view, respectively), from Bed 19, Selong Xishan section; (Z) *Hindeodus parvus*, from Bed 19, Selong Xishan section; (AA and BB) *Isarcicella staeschei* (oblique and upper view, respectively), from Bed 19, Selong Xishan section; (CC) *Hindeodus parvus*, from Bed 18, Selong Xishan section and (DD) *Hindeodus praeparvus*, from Bed 27, Qubu section.


A
B
C
D
E
F
G
H
I
J
K
L
M
N
O
P
Q
R
S
T
U
V
W
X
Y
Z
AA
BB
CC
DD
100μm

excursion in the lower part of the *Waagenites* Bed (Jin et al., 1996); the PTB as indicated by the FAD of the conodont *Hindeodus parvus* occurs immediately above the *Waagenites* Bed (Fig. 5Z, CC) although precise radiometric dating is not available. The overlying *Otoceras latilobatum* bed (Bed 18 in Fig. 4) is also condensed as a zonation can be recognized in the bed with rare *Hindeodus parvus* appearing in the lower third and *Isarcicella isarcica* appearing in the upper third (Orchard et al., 1994); as such it is possible that the PTB could be located within the lowermost part of this bed. This extinction interval as constrained by geochemical and biostratigraphical data can be precisely correlated with the end-Permian extinction at the Meishan section. It is worth mentioning that Changhsingian deposits are likely much thicker than that defined by Wang et al. (1989) because the Late Changhsingian conodonts *Mesogondolella sheni* and *Clarkina zhejiangensis* (the latter taxon was referred to both *C. taylorae* and *C. tulongensis*) occur in the top part of the Selong Group [the Coral Bed of Jin et al. (1996) and the pre-Changhsingian interval of Wang et al. (1989), Fig. 5A–D, H–I and R–S) at the Selong Xishan section (Xia and Zhang, 1992; Mei, 1996)].

A dramatic biofacies change occurred within the interval from the Coral Bed to the *Otoceras* Bed around the PTB (Fig. 2B). The Selong Group and the *Waagenites* Bed of the Kangshare Formation are dominated by brachiopods, corals, bryozoans and crinoids (Figs. 3L and 6A). Conodonts first occurred in the topmost part of the Coral Bed (including *Clarkina zhejiangensis*, *C. meishanensis*, *Mesogondolella sheni*, *Hindeodus* cf. *latidentatus*, *H. praeparvus*; Fig. 5) and became very prolific in the *Waagenites* Bed (*Clarkina zhejiangensis*, *Mesogondolella sheni*, *Hindeodus typicalis*, *H. praeparvus*) and the overlying *Otoceras* Bed (Yao and Li, 1987; Xia and Zhang, 1992; Orchard et al., 1994; Mei, 1996) (*Clarkina zhejiangensis*, *C. tulongensis*, *C. taylorae*, *C. orchardi*, *Mesogondolella sheni*?, *Hindeodus typicalis*, *H.* cf. *latidentatus*, *H. parvus*; Fig. 5). The similarity in conodont faunas in the Coral Bed and *Waagenites* Bed point to a minimal hiatus associated with the Caliche Bed that separates the two. Above the PTB, numerous ammonoids of varied sizes (Figs. 3M and 6H), ranging from centimetre to decimetre, are preserved on bedding planes, apparently indicating a faunal shift from diverse benthic to monotonous nektic taxa-dominated communities.

2.2. Microstratigraphical analysis

The PTB beds of the Selong Xishan section show a transition from crinoid grainstone in the topmost part of the Selong Group to compacted packstone corroded by stylolites in the basal part of the Kangshare Formation. Jin et al. (1996) subdivided them into five distinct beds based on their different fossil and sedimentary contents (Figs. 2B and 6). In ascending order they are the Coral Bed, the Caliche Bed, the *Waagenites* Bed, the *Otoceras* Bed and the *Ophiceras* Bed. The lithological changes across the PTB at the Selong Xishan section have been recently documented in detail by Wignall and Newton (2003).

The contact between the Selong Group and the Kangshare Formation is sharp (Fig. 6D) and marked by a Caliche Bed (Jin et al., 1996) with a crust-like structure (Fig. 6B and C). Wignall and Newton (2003) interpreted this bed as a stromatolite deposit with gypsum crystals in a hypersaline lagoon. However, our study of the same bed indicates that the bed is indeed a caliche with some "marine influence" as explained below. The classic interpretation for this kind of calcrete palaeosol implies subaerial exposure under a warm, semi-arid climatic setting frequently affected by sea water during a sea-level lowstand (Reeves, 1970; Walls et al., 1975).

The bed displays various textural attributes that point to "vadose" influence during the formation of multiple phases of laminated crusts. Dripstones or micro-stalactitic structures can be clearly seen extending downward from the top of the Caliche Bed (Fig. 6B). Numerous coated grains or glaebules can be seen below this surface and some of these white glaebules form coalesced masses around red-brown matrices (Fig. 7A and B). Intergrown with the micro-stalactitic structures are multiple generations of fibrous aggregates of calcite (possibly recrystallized from aragonite given the blunt terminations on the crystals: Fig. 6C); these crystallites clearly dissolve in dilute acid when isolated from the rock. The "stromatolites" interpreted and depicted by Wignall and Newton (2003; their fig. 5) are here re-interpreted as micro-stalagmitic structures at the base of the Caliche Bed. The mirror images of the convexity of these structures at the top and base of this bed suggest a common origin. In our view, the latter structures are displacive and not the product of a cyanobacterial column growing within the water of a hypersaline lagoon. Wignall and Newton (2003) reported gypsum in their sample, but we did not recognise this mineral within any of our thin-sections. There are distinct layers within the Caliche Bed as well that may point to some high-frequency climate induced sea-level fluctuations affecting the production of this "soil" at the margin of a Late Permian lowstand sea. Scholle and Kinsman (1974) described an aragonitic and high-Mg calcite caliche from a modern Persian Gulf supratidal sabkha

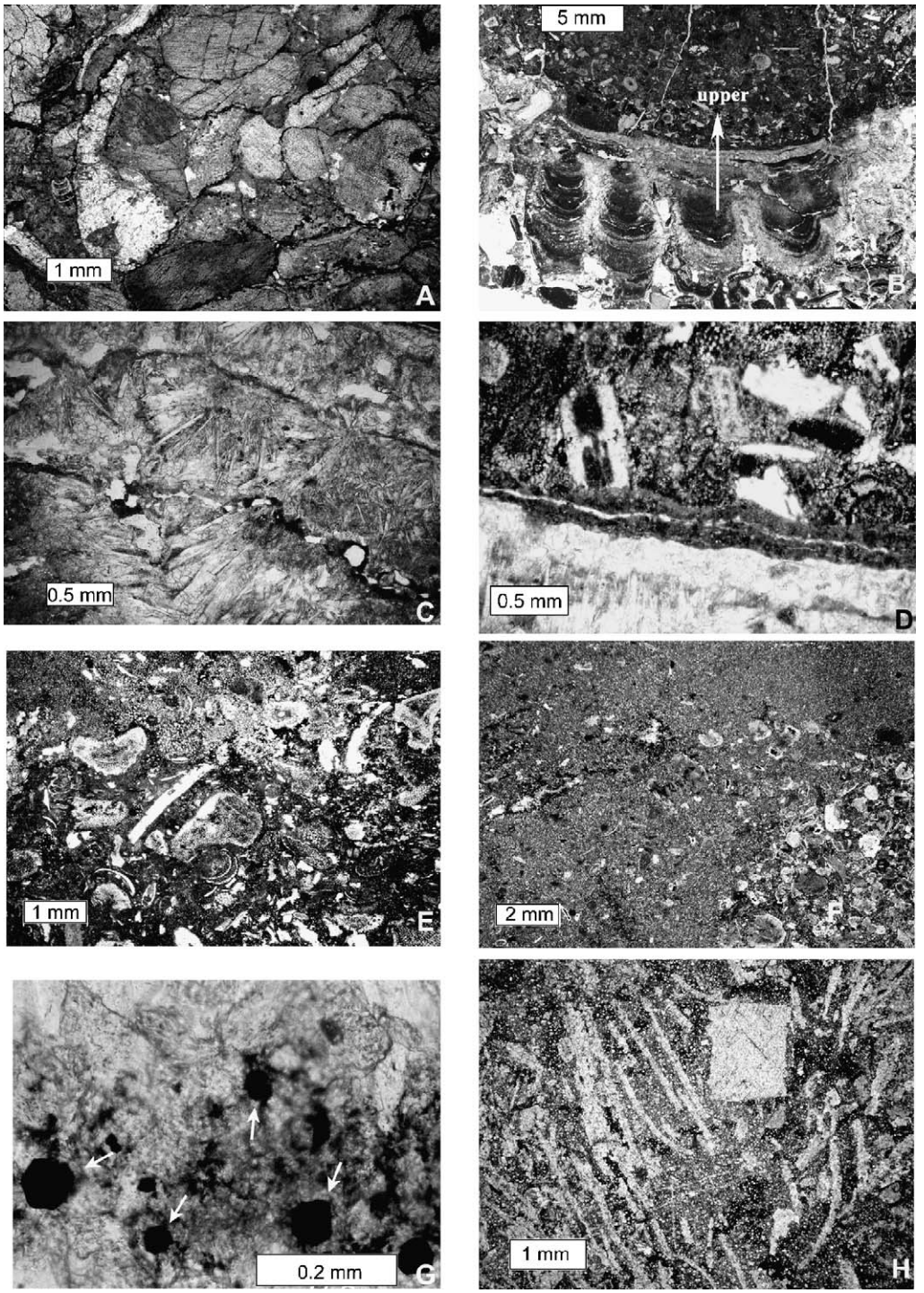

Fig. 6. Lithological sections of PTB beds at the Selong Xishan section. (A) Brachiopod grainstone of the Selong Group. (B) Micro-stalactitic structure of the Caliche Bed and overlying crinoid grainstone of the basal *Waagenites* Bed. (C) Needle-like aragonite recrystallised to calcite in the Caliche Bed. (D) Microphotograph showing the sharp contact between the Caliche Bed and the *Waagenites* Bed, note the dissolution of some bioclasts in the base of the overlying *Waagenites* Bed. (E) Various bioclasts dominated by echinoids associated with some brachiopods and tiny foraminifers between 2 and 7 cm above the Caliche Bed in the lower part of the *Waagenites* Bed. (F) Microphotograph of packstone in the lower part of the *Otoceras* Bed of the basal Kangshare Formation. (G) Common pyrite cubes (arrows) at about 23.5 cm above the PTB in the upper part of the *Otoceras* Bed of the basal Kangshare Formation. (H) Microphotograph showing numerous ammonoid shells at the level 33 cm above the PTB.

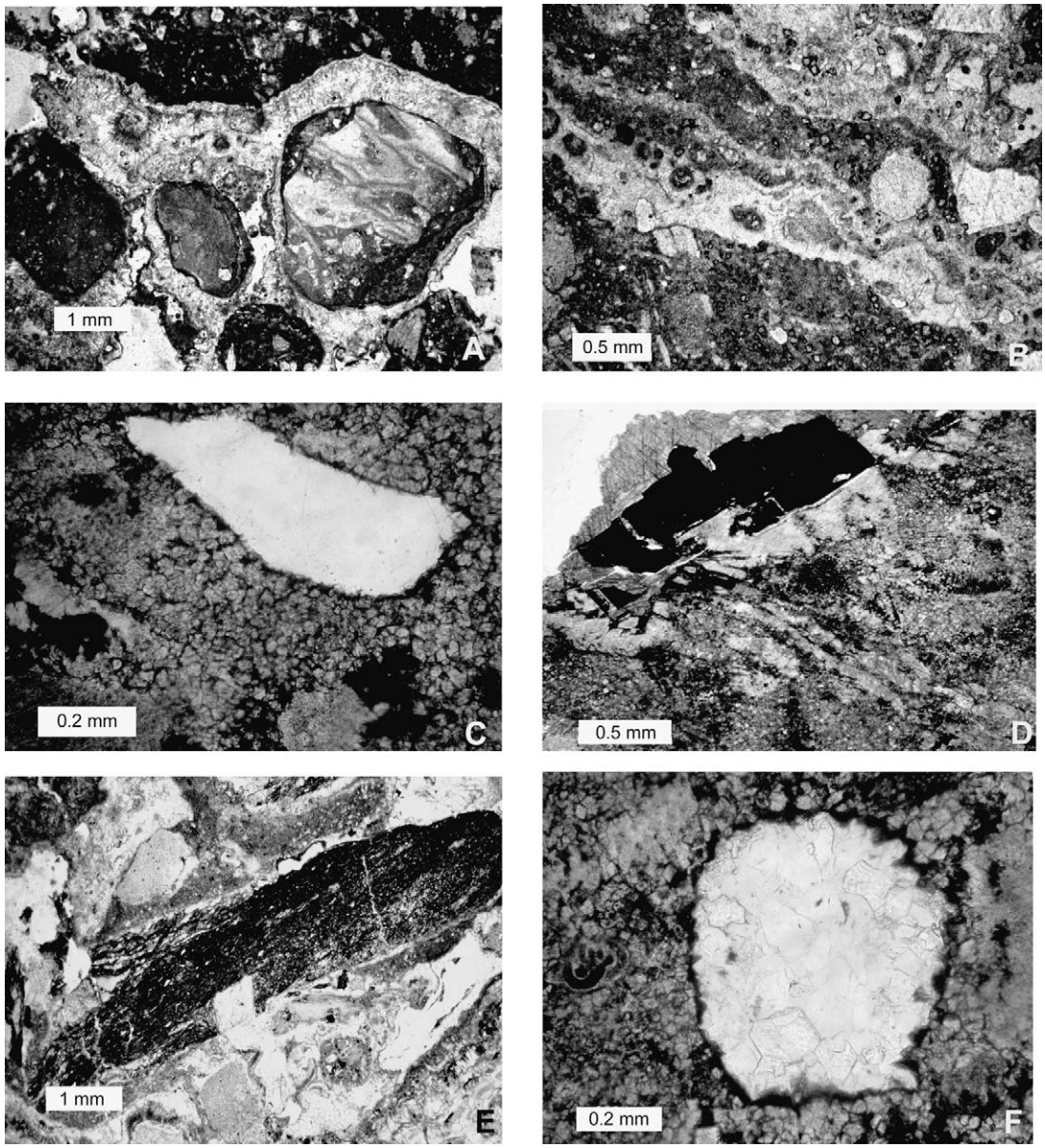

Fig. 7. Microphotographs showing terrigenous clasts in the Caliche Bed and the *Waagenites* Bed. (A) Coated intraclasts in the Caliche Bed. (B) Silt-sized quartz in the Caliche Bed. (C) Quartz grain in the *Waagenites* Bed. (D) Pyrite in the *Waagenites* Bed. (E) Silty shale grain in the *Waagenites* Bed. (F) Rock fragment in the *Waagenites* Bed.

setting that displayed textures typical of the vadose zone (see Estaban and Klappa, 1983; compare their figure 78 with our Fig. 6B), but with a vadose zone recharged not by freshwater, but by saline waters through any number of mechanisms including capillary action, wind-driven marine flooding, surf spray, or by Late Pleistocene-Holocene sea-level fluctuations. This mechanism can thus explain the development of a caliche with mineralogical characteristics suggestive of marine influence (Scholle and Kinsman, 1974). Furthermore, the carbon isotopes within the Caliche Bed support this marine influence. The lack of expected negative C-isotope values around −10 to −15 (see next section) that would be typical of meteoric freshwater diagenesis could have discounted the caliche interpretation without this model. In addition, small quartz grains and rock fragments (Fig. 7) and intraclastic brecciated material that are not present in any other adjacent beds including greenish-grey silty shale clasts mentioned by Wignall and Newton (2003) may be indicative of periodic exposure, reworking and

transportation associated with minor fluctuations of the shoreline during sea-level lowstand. There is no major time gap between the underlying Coral Bed and overlying *Waagenites* Bed since both are within the same conodont biozone indicated by *Clarkina meishanensis*, *C. zhejiangensis*, and *Mesogondolella sheni*, but despite the debate regarding the origin of the bed, the top of the Caliche Bed clearly marks a sequence boundary.

It follows therefore that a regression was likely to have culminated during deposition of the Caliche Bed. Above the Caliche Bed, a continuous polished section shows that the strata from the *Waagenites* Bed to the *Otoceras* Bed record a rapid deepening as indicated by a fining upward lithological shift from crinoid grainstone in the *Waagenites* Bed to thin-bedded stylo-compacted packstone in the overlying *Otoceras* Bed (Fig. 6). Algal microborings are present in the upper part of the *Waagenites* Bed. The *Otoceras* Bed is locally finely laminated and contains crinoid bioclasts. Bioturbation becomes weaker upward and pyrite crystals become common in the upper part of the *Otoceras* Bed (Fig. 6G).

2.3. Carbon and oxygen isotope geochemistry

The section was sampled in detail across the PTB. Carbon isotope ratios based on bulk rocks were determined by both the Nanjing Institute of Geology and Palaeontology and the Geological Survey of Canada using phosphoric acid evolution and subsequent mass spectrometry of evolved CO_2 with modification as necessary to deal with microdrilling to avoid possible weathered areas. The carbon excursion determined by the former was published in Jin et al. (1996). Herein we provided additional carbon and oxygen isotope results determined by the Geological Survey of Canada (Fig. 8).

Data from the Selong Xishan section determined by the two different labs show no substantial differences in carbon isotope values. The values from 2.16 m to about

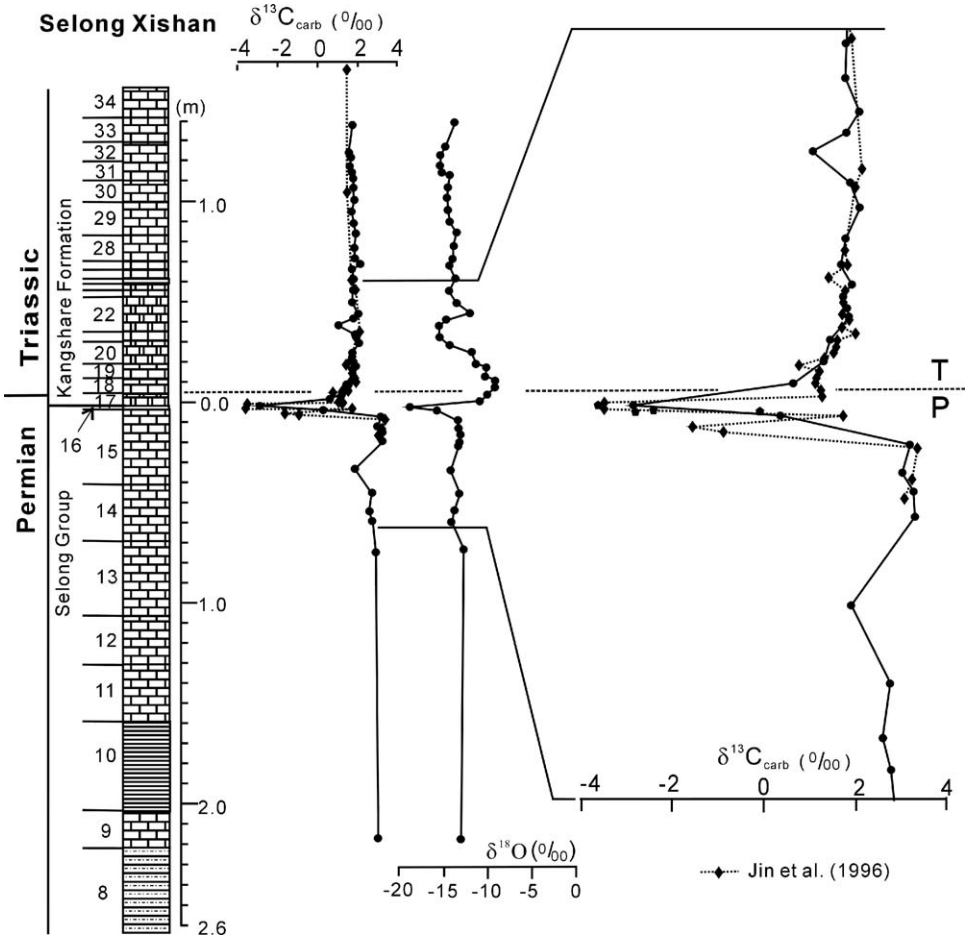

Fig. 8. Carbon and oxygen isotopic profiles around the PTB at the Selong Xishan section. The profile on the right is an expanded version of the carbon profile for the boundary interval. Carbon data come from two sources including new data and previously published data by Jin et al. (1996).

0.5 m below PTB remain fairly uniform between 2 and 3‰, which is within the range of those reported previously for Upper Permian rocks throughout the Palaeo-Tethys (e.g. Margaritz et al., 1988). At the level of 35.5 cm below the PTB, $\delta^{13}C_{carb}$ values dropped to 1.93‰, then recovered to 3.20‰ at 11.5 cm below the PTB, followed by a sharp drop to −2.89‰ at 5.5 cm below the PTB within the lower part of the *Waagenites* Bed. Similar sharp negative shifts occur at many previously studied sections in the world, although they have different magnitudes and stratigraphic levels around the PTB (Margaritz et al., 1988; Holser et al., 1989; Baud et al., 1989; Wang et al., 1994; Jin et al., 2000; Twitchett et al., 2001). The very sharp drop as exhibited at Meishan (Jin et al., 2000) and Selong (this study), in contrast to somewhat more gradual changes at Gartnerkofel (Holser et al., 1989), is probably related to either extreme condensation or the presence of a minor hiatus or both. The segment with double drops in $\delta^{13}C_{carb}$ values near the PTB at the Selong Xishan section can be well correlated, respectively, with those in Bed 24e at the Meishan section (Jin et al., 2000; Cao et al., 2002) and those in the Mazzin Member of the Werfen Formation in the Gartnerkofel core in the Carnic Alps of Austria (Holser et al., 1989). The $\delta^{13}C_{carb}$ values recovered to 1.32‰ at 1.5 cm into the *Otoceras* Bed and 1.81‰ at 10 cm above the PTB. The accompanying values of δ18O also show remarkably consistent variations (−8.89 to −18.76‰) in the same intervals although they are far too depleted compared with both the previously published data and the "theoretical" values determined in other regions; these differences may reflect the effect of diagenesis. They are centred at −18.76‰ at 5.5 cm below the PTB (Fig. 8). The negative $\delta^{13}C$ excursion in carbonate is also consistent with that in organic $\delta^{13}C$ excursion in other PTB sections (e.g. Wang et al., 1994; Krull and Retallack, 2000; Twitchett et al., 2001).

Except for the above-mentioned two sets of samples, we have also especially analysed two additional sets of carbon isotope ratios based on bulk rocks of the Caliche Bed and the *Waagenites* Bed to determine whether the Caliche Bed is composed of primary carbonate formed in a marine environment during the latest Permian or "secondary" carbonate generated by subsequent HCO_3-precipitates. The values of the rocks below the "Caliche Bed" are typically around +3‰, and those above in the Triassic are about +1.8‰. The $\delta^{13}C_{carb}$ values of four different samples of the Caliche Bed are −2.543, −0.104, 1.776 and 0.35‰. They are all within the range of values exhibited by the PTB negative shift and not as negative as would be expected if they were a secondary carbonate resulting from freshwater diagenesis.

3. Qubu section

The Qubu section, about 30 km north from Mt. Everest, is well exposed in the northwestern side of the Zaga River (Fig. 2C). Lopingian strata at this section have been subdivided into the Qubu and Qubuerga formations in ascending order based on lithological characteristics (Yin and Guo, 1979; Shen et al., 2003b). The upper Qubuerga Formation is separated into two lithologic members.

3.1. Faunal shift

The lower member of the Qubuerga Formation is characterised by grainstone, calcareous mudstone and siltstone with numerous brachiopods, bryozoans and some solitary corals and ammonoids (Fig. 9A and B). Brachiopods have been studied in detail and two brachiopod assemblages have been recognised (Shen et al., 2003b), of which the lower assemblage is Wuchiapingian and the upper assemblage may be partly Changhsingian (Shen et al., 2003b). Gastropods become more common from Bed 18 of the lower member of the Qubuerga Formation, and are dominated by *Callistadia* species.

There are no brachiopods in the upper (Nimaluoshenza) member. However, gastropods (Pan et al., in preparation), including *Bellerophon*, *Retispira* and *Naticopsis* (*Jedria*), and numerous bivalves dominated by *Atomodesma variabilis* are very abundant in the lower part of the Nimaluoshenza Member. The gastropod genera are mostly wide-ranging and biogeographically mixed forms (i.e. there are forms characteristic of both palaeoequatorial and Gondwanan realms and also forms typical of North America). The faunal shift (Fig. 10) from brachiopod-dominated to bivalve- and gastropod-dominated assemblages is associated with distinctive facies changes (see lithological changes below). The upper part of the Nimaluoshenza Member of the Qubuerga Formation contains abundant spores and pollen dominated by Permian pteridophytes and Late Permian acritarchs (Fig. 9D; Lu, personal communication). The topmost 50 cm (Fig. 2D) of the Qubuerga Formation is of interest because it contains numerous poorly preserved thin-shelled ammonoids, signaling a shift from benthic communities in the underlying parts of the Qubuerga Formation to the nektic taxa-dominated communities. This ammonoid-dominated assemblage continued into the overlying dolostone unit (Fig. 2C and D) of the Tulong Formation. However, numerous conodonts, dominated by *Clarkina tulongensis*, *C. taylorae*, and *C. orchardi*, began to occur in Bed 27 of the dolostone unit (Fig. 5). A few fragments of the conodont

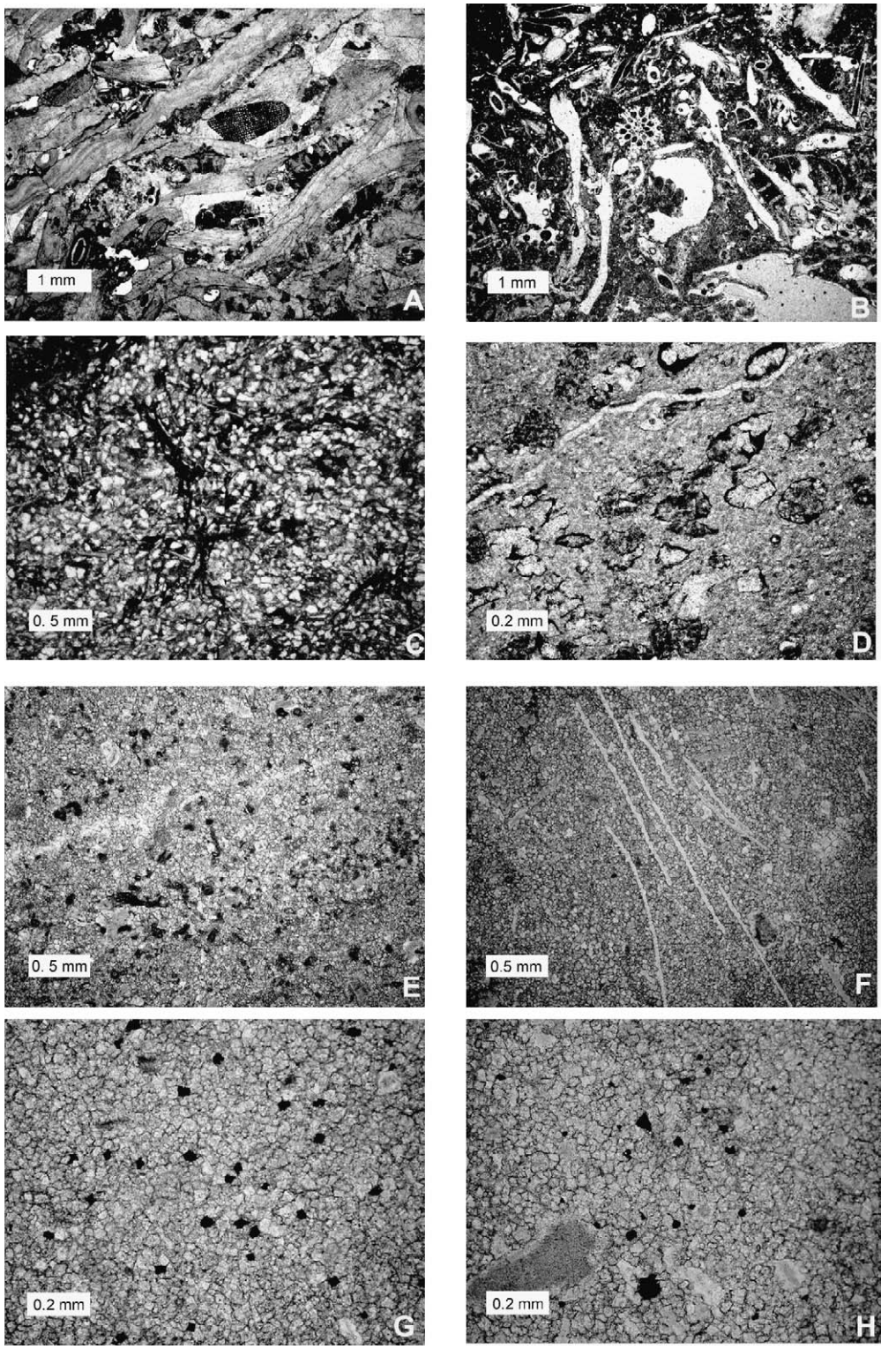

Fig. 9. Lithological sections of PTB beds at the Qubu section. (A and B) Brachiopod and bryozoan grainstone from the topmost part of the lower member of the Qubuerga Formation. (C) Siltstone with abundant fine quartz grains and some mica in the Nimaluoshenza Member of the Qubuerga Formation. (D) Abundant acritarchs in the upper part of the Nimaluoshenza Member (about 5 m below the PTB). (E) Abundant tiny foraminifers in Bed 25. (F) Abundant ammonoid shells in Bed 27. (G) Abundant pyrite cubes in Bed 25. (H) Abundant pyrite cubes in Bed 27.

Hindeodus cf. *parvus* were found from Bed 33 (Fig. 5) suggesting that the PTB is low within the dolostone unit, but not at the base. No Permian brachiopods like the mixed fauna in the PTB beds in South China are found from the dolostone unit, implying an earlier disappearance pattern. Here we consider that this earlier pattern of faunal changeover is most likely related to facies exclusion.

3.2. Microstratigraphical analysis

The topmost part of the lower member of the Qubuerga Formation consists of brachiopod/bryozoan grainstone (Fig. 9A and B) containing some silty quartz, feldspar and shale clasts. Brachiopod and bryozoan fragments occupy about 95% of the bioclasts, suggesting a high-energy shallow shoal environment. Other rare bioclasts include corals and crinoids. Quartz grains are all rounded or subrounded. Zircon and apatite can be seen in addition to the quartz grains, indicating that they were transported from the nearby lands.

The Nimaluoshenza Member of the Qubuerga Formation (Fig. 10) is characterised by siltstone and silty shale (Fig. 9C) topped with 50 cm vari-coloured shale (Fig. 2D). The lower part of this member is composed of carbonaceous siltstone and siliceous mudstone containing radiolarians. Gastropod shells are all silicified. Lithoclasts mainly consist of quartz, white and black mica (Fig. 9C). Upward, the lithology changes to black siltstone and shale until the vari-coloured shale with numerous ammonoids occurring in the top 50 cm of the Qubuerga Formation. The vari-coloured shale may

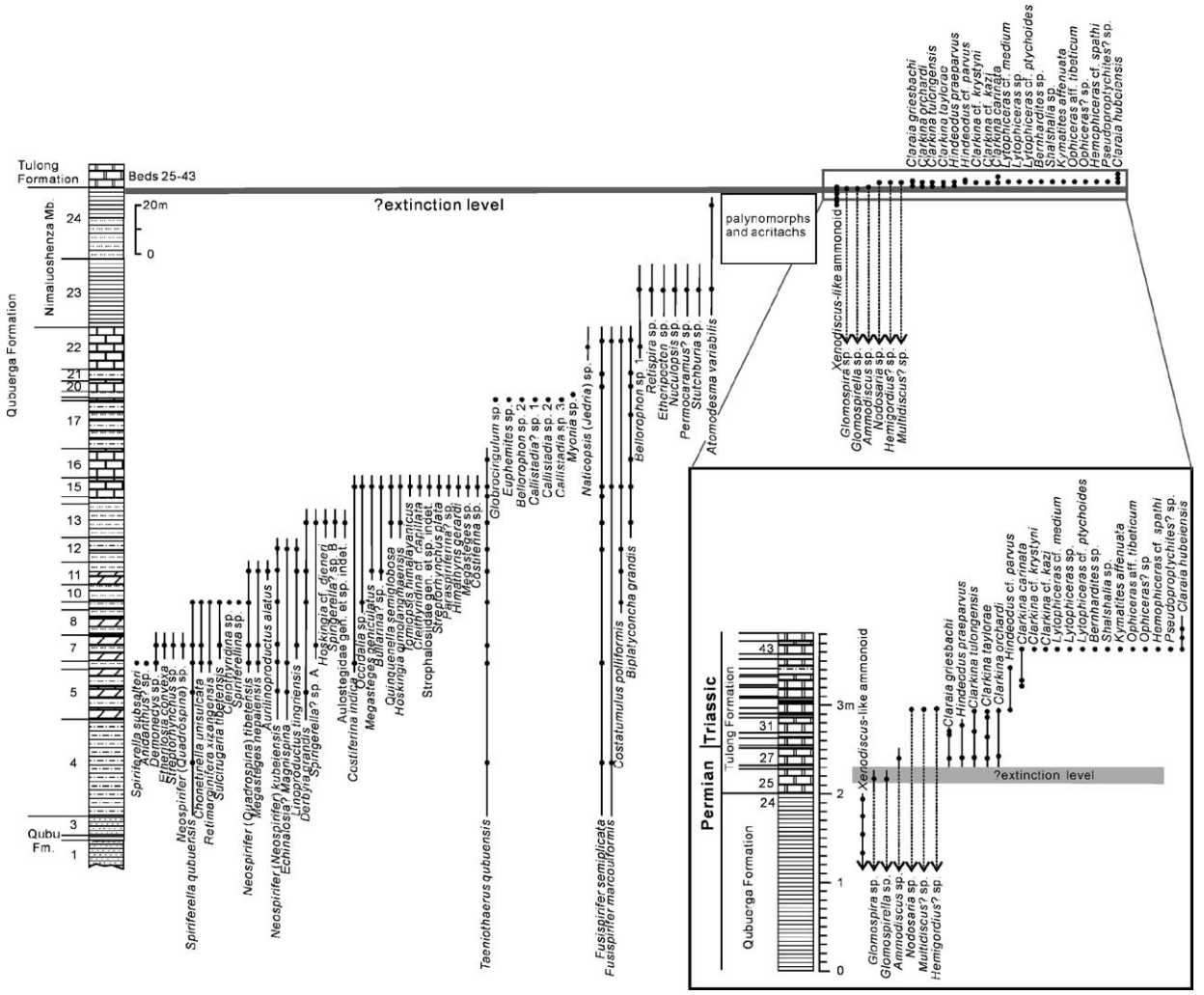

Fig. 10. Composite range chart of various fossils at the Qubu Section.

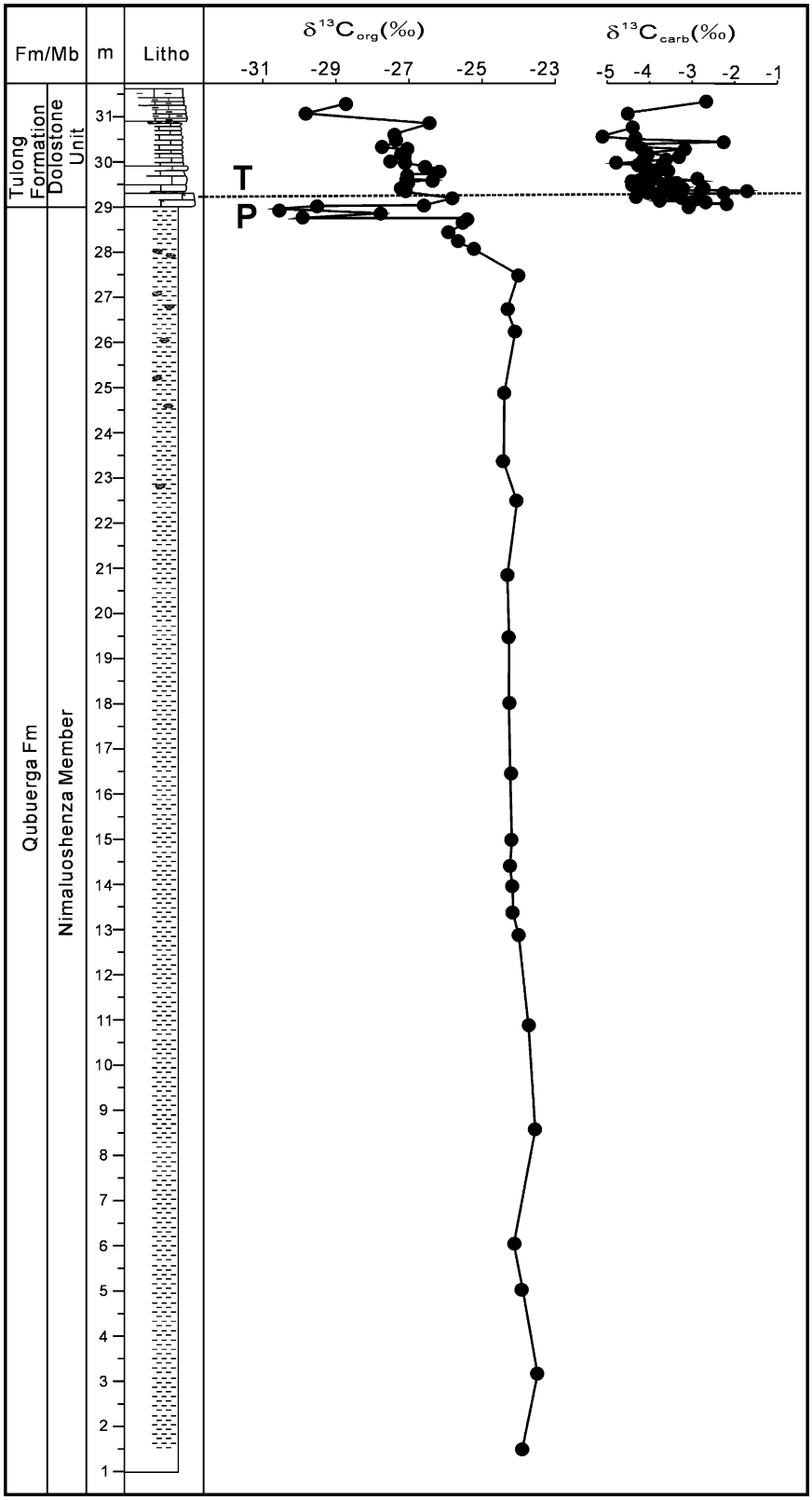

Fig. 11. $\delta^{13}C_{carb}$ and $\delta^{13}C_{org}$ profiles around the PTB at the Qubu section.

be indicative of periodic exposure within an intertidal-supratidal setting with ammonoids concentrating along a palaeo-shoreline. The contact between the Qubuerga Formation and overlying dolostone unit of the Tulong Formation is sharp (Fig. 2D), but this does not seem to point to a significant hiatus because the same ammonoid assemblage is present in both the Qubuerga Formation and the overlying Tulong Formation.

A detailed lithological study indicates that the medium-bedded dolostone unit is mainly composed of dolomitic wackestone interbedded with a few mudstone beds of 2–3 cm thickness. The dolomitic wackestone contains numerous small foraminifers (Fig. 9E), some bivalves, ammonoid shells (Fig. 9F) and rare crinoids. Pyrite cubes are abundant in Bed 27 in the lower part of the dolostone unit (Fig. 9G and H). All the foraminifers are micritised. The sharp base of the dolostone unit and other textural attributes described above may point to a transgressive erosion surface and onlapping shallow ramp carbonate deposits. Above Bed 27, the remainder of the dolostone unit at the Qubu section consists of recrystallised dolostone with abundant well oriented ammonoid shells and rare crinoid fragments (Fig. 9F).

3.3. Carbon isotope geochemistry

The section was extensively sampled from the uppermost part of the lower member of the Qubuerga Formation to the topmost bed of the dolostone unit of the Tulong Formation. In total, 103 samples were collected and analysed. The samples from the black shale of the Nimaluoshenza Member were sampled based on depth, while the samples of the dolostone unit were collected bed by bed. Organic and inorganic carbon isotopes were analysed by the Nanjing Institute of Geology and Palaeontology. Since the Nimaluoshenza Member of the Qubuerga Formation consists of black shale and siltstone, no reliable results of $\delta^{13}C_{carb}$ are available. Only two samples from the underlying Bed 23 give the values of −1.3 and 0.27‰. However, the accompanying oxygen isotope values are both below −15‰, indicating the samples had been influenced by subsequent diagenesis. $\delta^{13}C_{carb}$ values from the dolostone unit of the Tulong Formation all slightly fluctuated at a value of about −4‰, but no sharp drop was detected, suggesting that the sharp drop slightly below the PTB in other sections in the world is likely within the underlying black shale of the Nimaluoshenza Member (Fig. 11).

Organic carbon isotope data show that the values in the black shale and siltstone remain steady at about −24‰ until the topmost part of the member. The profile of the organic carbon isotope displays that the values at the level of 1.5 m below the dolostone unit of the Tulong Formation begin to decrease gradually below −25‰. Two sharp drops with respective values of −30.1 and −30.66‰ occur in the vari-coloured shale of the topmost 25 cm of the Qubuerga Formation (Fig. 11). The negative depletions of $\delta^{13}C_{org}$ have magnitudes of 4.7 and 3‰ for the two drops. The organic carbon isotope values immediately shift back to −26.6‰ in the basal part of the dolostone of the Tulong Formation and remain steady at about −27‰ in the following 2 m of the dolostone unit, which is followed by a minor decrease with values ranging between −29.8 and −28.74‰ (Fig. 11).

The gradual depletion of $\delta^{13}C_{org}$ in the uppermost part of Unit 24 of the Qubu section is generally comparable with that below Bed 23 of the Meishan D Section (Cao et al., 2002, fig. 2). The following gradual and sharp drops associated with the burst of abundant ammonoids are respectively correlated with the two drops in Beds 23–24 and Bed 26 at the Meishan Section (Cao et al., 2002).

4. Tulong section

4.1. Lithology

The Tulong section is situated about 60 km west of the Qubu section. The PTB section is exposed at Nimaluoshenza about 2 km south of Tulong village (Fig. 1C). The P–T sequence consists of the Qubu Formation, Qubuerga Formation and the Tulong Formation in ascending order; these units are readily correlated with lithologic equivalent units at the Qubu section. The upper member of the Qubuerga Formation was named the Nimaluoshenza Member by Rao and Zhang (1985). This member is overlain by the dolostone unit of the Tulong Formation.

4.2. Faunal shift

Abundant brachiopod fossils were collected from the siltstone, bioclastic limestone and mudstone in the lower member of the Qubuerga Formation (Shen et al., in preparation). The brachiopod fauna is comparable to the fauna from the lower member of the Qubuerga Formation at the Qubu section as indicated by many species that are common to both sections: *Retimarginifera xizangensis*, *Biplatyconcha grandis*, *Costiferina indica* and *Quinqunella semiglobosa* (Fig. 12).

Two of the authors (SSZ and CCQ) visited the PTB sections in 1994 and 1998, unfortunately the trench dug by Rao and Zhang (1985) had disappeared due to rapid weathering. According to the evidence from

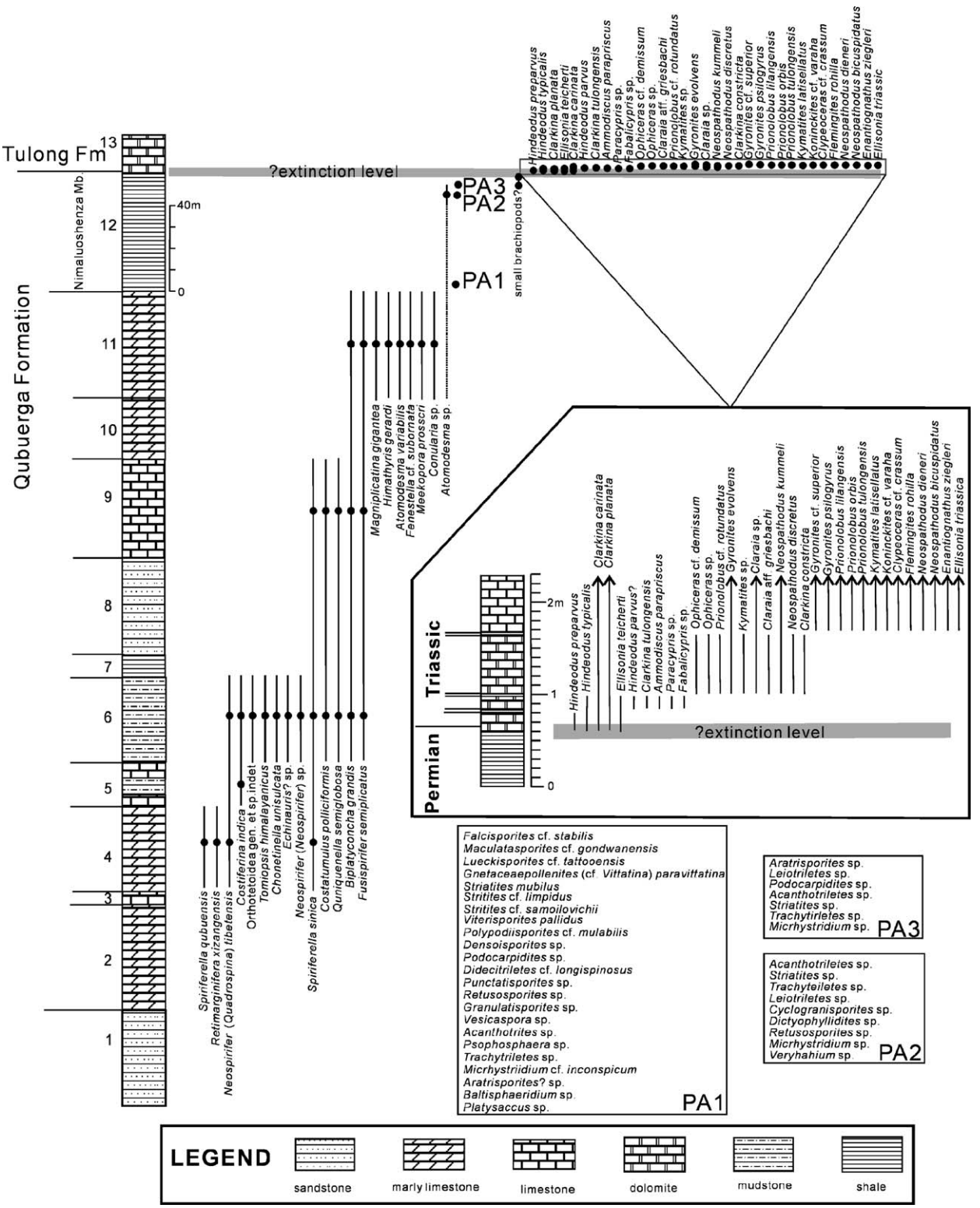

Fig. 12. Composite range chart of various fossils at the Tulong section. Data from Tian (1982), Rao and Zhang (1985) and Shen (in preparation).

shale clasts from the Nimaluoshenza Member in outcrop and the description of Rao and Zhang (1985), the brachiopods disappeared in the Nimaluoshenza Member, and the bivalve *Atomodesma variabilis* is very common in the level about 10 m below the dolostone unit. The palynological analysis by Rao and Zhang (1985) showed that the Nimaluoshenza Member yielded abundant palynomorphs and acritarchs (Fig. 12). The pollen-dominated palynological assemblage indicates a Permian-Triassic mixed character as indicated by the presence of *Aratrisporites* sp. and many other common elements in the Permian-Triassic transition. According to Rao and Zhang (1985), the black shale around 60 cm below the top of the Nimaluoshenza Member yields some small unidentifiable brachiopods and arthropods. The topmost 60 cm of the member also consists of varicoloured shale, which is the same as that at the Qubu section.

The overlying dolostone unit of the Tulong Formation contains abundant conodonts (Tian, 1982). *Hindeodus praeparvus*, *H. parvus*, *Clarkina carinata* and *C. planata* occur immediately above the Nimaluoshen Member. A foraminifer identified as *Ammodiscus parapriscus* and the ostracods *Paracypris* sp. and *Fabalicypris* sp. have been recorded from the lower part of the dolostone unit. The conodont assemblage is correlatable with that in the dolostone unit at the Qubu section although the conodont taxonomy needs to be revised based on new taxonomic knowledge for other peri-Gondwanan sections. Abundant ammonoids dominated by *Ophiceras* and the bivalve *Claraia* first occur at a level about 34 cm above the bottom of the dolostone unit (Rao and Zhang, 1985).

5. Other sections in the peri-Gondwanan region

5.1. The Salt Range, Pakistan

The biostratigraphy of the PTB section in the Salt Range, Pakistan has been extensively studied (Kummel and Teichert, 1970; Sweet, 1970; Pakistan-Japanese Working Group (PJWG), 1985). However, whether or not the Permian-Triassic contact in the Salt Range is continuous and whether the Changhsingian is present or absent has been the focus of dispute for a long time. Sweet (1970) considered the Permian-Triassic boundary to be a paraconformity with the latest Permian and earliest Triassic unrepresented. However, Sweet (1992) considered the strata previously assigned to the topmost Permian Changhsingian stage to be contemporary with the basal Triassic based on graphic correlation. Grant (1970) considered the brachiopod-bearing basal part of the Kathwai Member of the Mianwali Formation to be Guadalupian in age. However, due to recent revised conodont taxonomy (Mei et al., 1999; Wardlaw and Mei, 1999; Mei and Henderson, 2002, table 1), the stratigraphic correlations have been significantly improved. The Capitanian/Wuchiapingian boundary is approximately one-third up in the Wargal Formation. *Clarkina longicuspidata* occurs in the upper Wuchiapingian and lowest Changhsingian (Wardlaw and Mei, 1999). Its last occurrence in the lower half of the Chhidru Formation at the Zaluch Nala section is very close to the boundary between the Wuchiapingian and Changhsingian. Thus, the Changhsingian is more than 30 m thick at Zaluch Nala based on the measurement of PJWG (1985). The upper part of the Chhidru Formation is characterised by some typical cool-water conodonts such as *Vjalovognathus* sp. and *Merrillina* sp. and some bellerophontid gastropods. The lower Kathwai Member yields *Clarkina meishanensis* at its base followed closely by the FAD of *Hindeodus parvus* and *Isarcicella isarcica* and *Clarkina carinata* at the top and in the overlying lower part of the Mittiwali Member (Wardlaw and Mei, 1999). Therefore, the PTB is placed between the Kathwai Members A and B (L and M in Fig. 13) (PJWG, 1985; Wignall and Hallam, 1993; Wardlaw and Mei, 1999).

Diverse brachiopods including 22 species within 20 genera from the White Sandstone Unit in the topmost Chhidru Formation and 14 species within 13 genera from the basal Kathwai Member A were described by Grant (1970). These brachiopods were partly renamed by Waterhouse and Gupta (1983). Among the 14 species in the basal Kathwai Member, 13 species apparently range from the underlying strata. Only *Crurithyris extima* may be new to the interval. Seven species including *Spinomarginifera kathwaiensis*, *Martinia acutomarginiformis* and *Linoproductus periovalis* are shared by the White Sandstone Unit and the Dolomite Unit of the Kathwai Member, probably implying a very minor hiatus at most between the White Sandstone Unit and the Kathwai Member. The brachiopods in the White Sandstone Unit are dominated by typical warm-water palaeoequatorial genera such as *Enteletes*, *Leptodus* and *Richthofenia* associated with the bipolar and bi-temperate genus *Waagenoconcha*. In contrast, the brachiopods in the basal Kathwai Member are all characterised by warm-water Tethyan-type or cosmopolitan genera. Many typical Gondwana-type genera such as *Costiferina*, *Taeniothaerus*, *Spiriferella* and *Waagenoconcha*, common in the underlying Amb, Wargal and Chhidru formations, had completely disappeared by the Kathwai Member (Fig. 13).

PJWG (1985) and Mertmann (2000) studied in detail the foraminifer succession in the Salt Range, Pakistan.

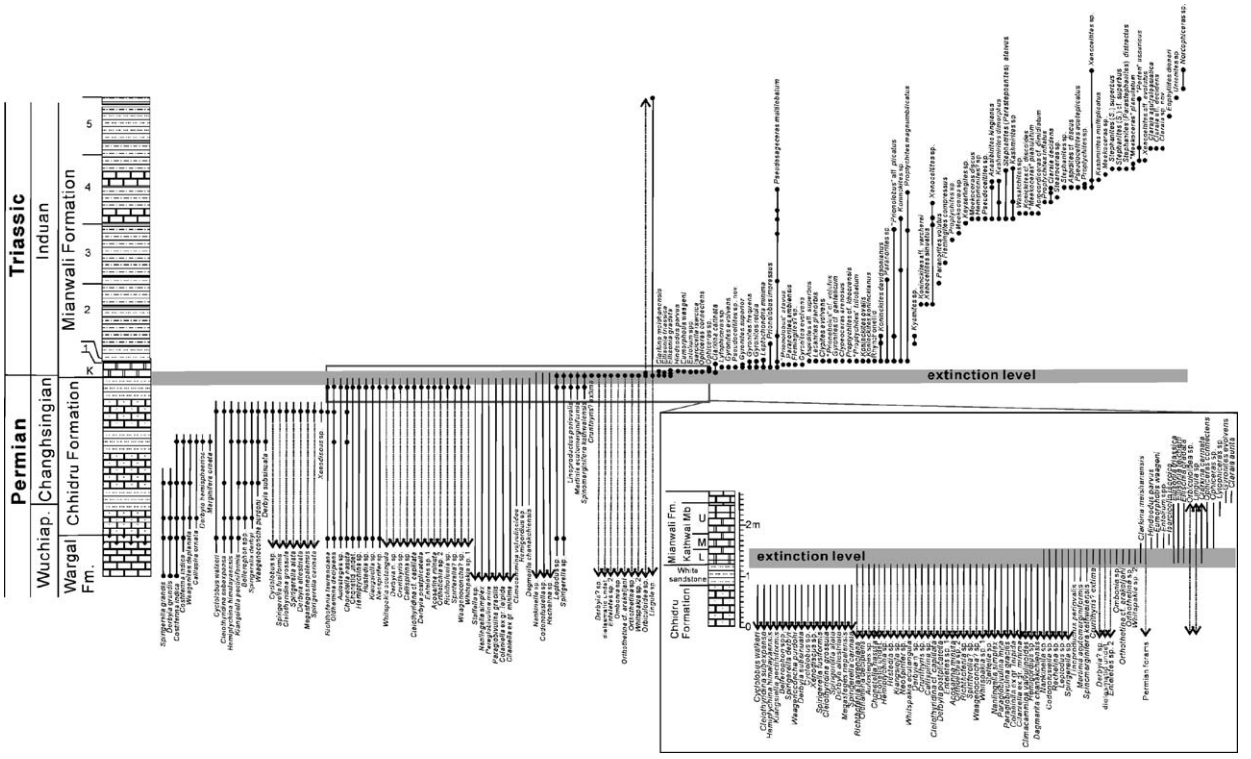

Fig. 13. Composite range chart of various fossils in the Salt Range sections. Data from Grant (1970), Kummel and Teichert (1970), Waterhouse and Gupta (1983), PJWG (1985), Wardlaw and Mei (1999) and Mertmann (1999, 2000, 2003). K, Kathwai member.

The upper Chhidru Formation contains a characteristic *Colaniella*-dominated fauna. Four fusulinid and eight small foraminifer species disappeared in the topmost part of the White Sandstone Unit of the Chhidru Formation. Only three species, including *Nankinella* sp., *Codonofusiella* sp. and *Reichelina* sp., disappeared in the basal part of the Kathwai Member A (Mertmann, 2000, fig. 3).

The White Sandstone Unit has been interpreted as having been deposited in a shallow subtidal to intertidal area with freshwater influences (Mertmann, 2003) as indicated by an increased terrigenous input of coarse-grained sandy material. The boundary between the Chhidru and Mianwali formations is interpreted as a sequence boundary with erosion and hiatus in the uppermost Permian (Haq, 1987; Mertmann, 1999). The Kathwai Member represents three thin retrogradational parasequences separated by flooding surfaces (Wignall and Hallam, 1993).

Carbon isotope values for the P–T transition in the Salt Range, Pakistan show broad similarities with that for the Selong Xishan and Qubu sections. $\delta^{13}C_{carb}$ values in the Late Wuchiapingian and Early Changhsingian lower Chhidru Formation are about +4‰ (Baud et al., 1996). The carbon isotopic values decrease from the middle part of the Chhidru Formation and the drop accelerates smoothly at the top of the Chhidru Formation until about +2‰. Low negative records occur in the lower part of the Kathwai Member, which is followed by a positive excursion of about +1.5‰ in the middle and Upper Kathwai Member of Early Induan age (Baud et al., 1996).

5.2. Kashmir

As in the Salt Range, Pakistan, the PTB sections in Kashmir have also been well known for continuous sedimentation along the northern passive margin of Gondwana. Nakazawa et al. (1975), Nakazawa (1981, 1993), Matsuda (1981, 1982, 1983a,b) and Kapoor (1992, 1996) have published extensive biostratigraphical data. Stratigraphic units, sequences and fossil ranges are plotted in Fig. 14.

As shown in Fig. 14, the *Colaniella*-dominated fauna in Member A of the Zewan Formation has restricted the formation to a Lopingian age. The brachiopods in the Zewan Formation, characterised by *Costiferina indica*, *Larmnimargus himalayaensis* and *Cleiothyridina* aff. *subexpansa*, provide a general correlation with those of the Lopingian of the Salt Range, Pakistan and the Selong

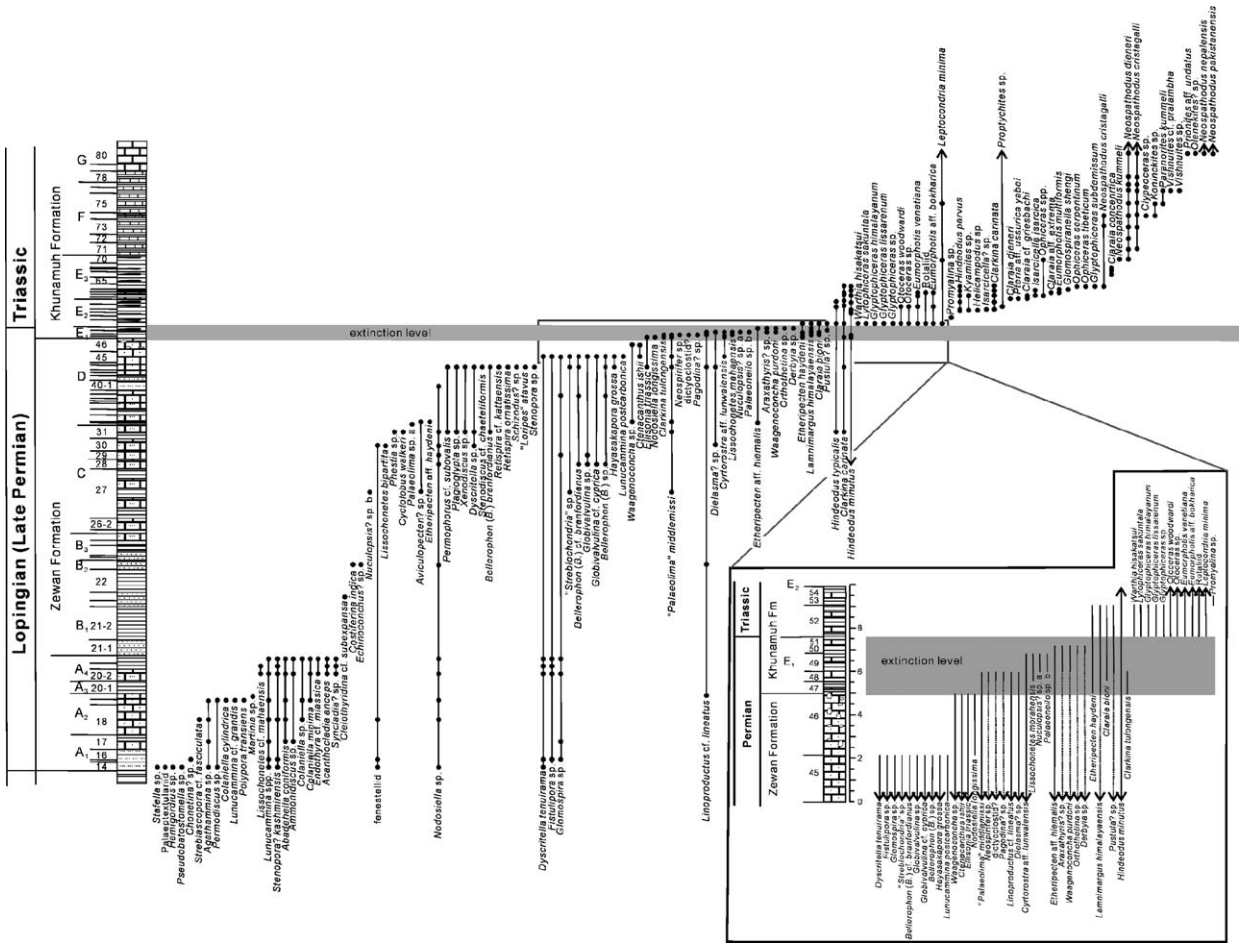

Fig. 14. Composite range chart of various fossils in Kashmir. Various taxa have been updated based on the latest information. Data from Nakazawa et al. (1975), Matsuda (1981, 1982, 1983a,b), Nakazawa (1981, 1993) and Kapoor (1992, 1996).

Group in southern Tibet. The middle part of Member C of the Zewan Formation yields the ammonoid *Cyclolobus walkeri* and *Xenoaspis* sp. (Nakazawa et al., 1975). The occurrences of *Cyclolobus* in the Salt Range are in the Kalabagh Member of the topmost Wargal Formation and the lower part of the Chhidru Formation, which is Late Wuchiapingian or Early Changhsingian. The overlying Member D of the Zewan Formation is likely Changhsingian and contains abundant brachiopods, bryozoans, foraminifers and gastropods including *Bellerophon* (*Bellerophon*) *branfordianus*, *Retispira ornatissima* and *Retispira* cf. *kattaensis* (Nakazawa et al., 1975; Kapoor, 1992). Permian brachiopods including 11 species and some bivalves and foraminifers continue to be present in Unit E_1 of the Khunamuh Formation. This unit, which is immediately overlain by the *Hindeodus parvus* Zone, is therefore apparently latest Changhsingian in age. Many Triassic taxa including four ammonoid species of *Otoceras* and *Glyptophiceras* and five bivalve species of *Claraia* and *Eumorphotis* occur in the overlying Unit E_2 of the Khunamuh Formation, suggesting that the faunal turnover happened just below the PTB as defined by the FAD of *Hindeodus parvus* (Fig. 14). Only two brachiopod species (*Pustula*? sp. and *Larmnimargus himalayaensis*) and a bivalve species (*Etheripecten haydeni*) continue to be present as relics in Bed 52 of Unit E_2 (just as Permian brachiopods extend a little higher in Meishan up to Bed 28 as seen in Jin et al., 2000); Permian brachiopods totally disappeared thereafter. It is also worth mentioning that some warm-water Tethys-type brachiopods such as *Orthothetina* sp. and *Ombonia* sp. occur in Unit E_1 of the Khunamuh Formation in Kashmir (Shimizu, 1981).

Lithologically, the Zewan Formation is composed of carbonate rocks accompanied by sandy shale (Member A), shale and carbonate-poor rocks (Member B), rhyth-

mic alternation of calcareous sandstone and sandy shale with shale predominant (Member C) and thick-bedded sandy limestone and sandy shale along with muddy sandstone in the lower part and calcareous as well as muddy sandstone in the upper part (Member D) (Kapoor, 1996). The lithology and fauna of Unit C suggests a neritic to shallow bathyal environment and later a restricted environment may be developed as indicated by the tendency toward dwarfing of brachiopods (Kapoor, 1992; Brookfield et al., 2003). The uppermost Member D of the Zewan Formation suggests uplift of the land and/or shallowing of the sea (Kapoor, 1992). Therefore, the topmost part of the Zewan Formation apparently represents a sequence boundary. The transgression beginning from the bottom of Unit E_1 of the Khunamuh Formation is marked by the rapid change from the Zewan Formation sandstone to the Khunamuh Formation shale, a dramatic decrease in quartz sand and an increase in mud (Brookfield et al., 2003).

The carbon isotope curve (Baud et al., 1996) shows similarities with those of the Salt Range, Selong and many other PTB sections in the world. The carbon isotope values during the deposition of the Zewan Formation remained stable, followed by a sharp drop in the basal Khunamuh Formation. This sharp drop is slightly before the disappearance of the diverse latest Changhsingian macrofauna that is characterised by the invasion of some warm-water elements (e.g. brachiopods and some conodonts).

6. Discussion

6.1. Synchronous extinction level compared with Meishan section in South China

As documented in the above five sections in the peri-Gondwanan region, the upper level of the mass extinction interval is very close to the PTB defined by the FAD of *Hindeodus parvus* (Fig. 15). A rapid extinction occurs just below or at the PTB. This extinction event may extend as a tail into the very earliest Griesbachian (Induan) as suggested by extinctions in Bed 52

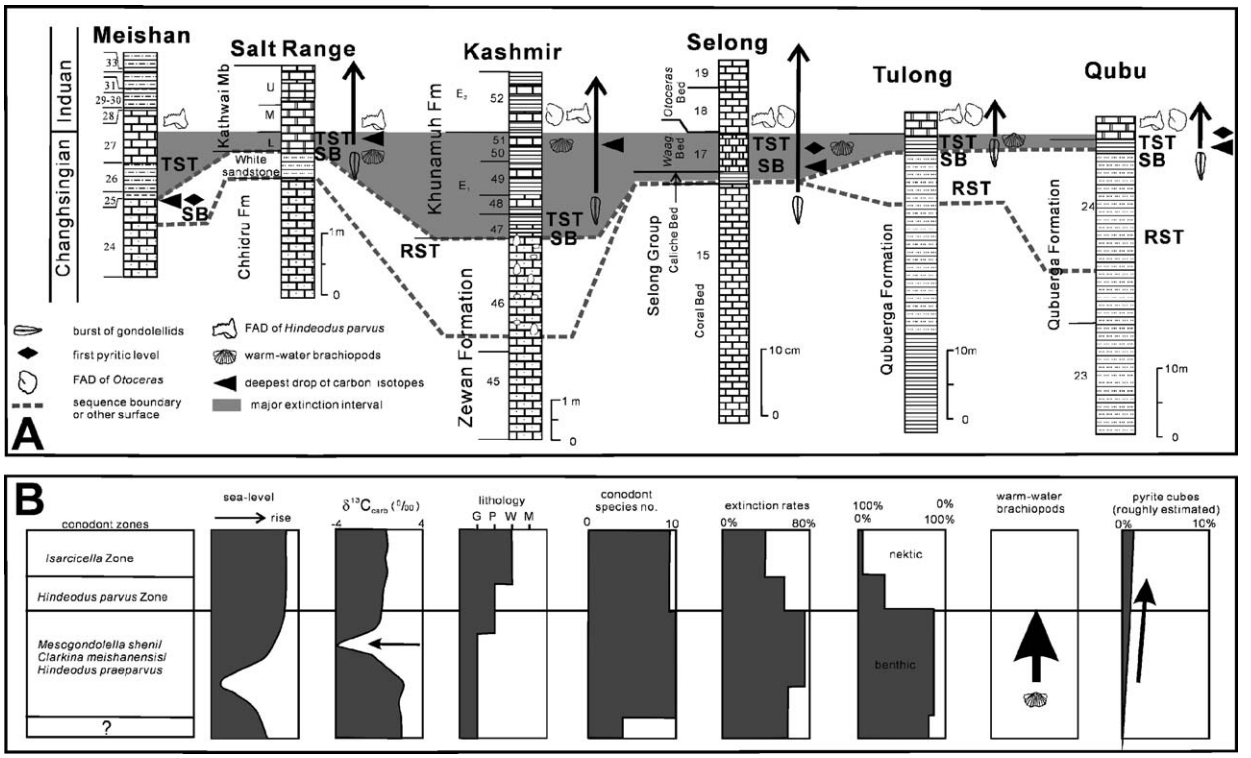

Fig. 15. (A) Comparison of extinction interval of five sections in the northern peri-Gondwanan region based on biostratigraphic, sequence stratigraphic and geochemical data. (B) Generalised geologic changes across the Permian-Triassic boundary in the peri-Gondwanan region. Sea-level, lithology, carbon isotope, benthic/nektic ratios are largely based on the Selong Xishan section; extinction rates calculated based on Kashmir, the Salt Range and Selong Xishan sections; pyritic cube contents are approximate based on estimation under microscope; conodont abundance based on all sections. Sequence terminology after Embry and Johannessen (1992).

at Kashmir and Bed 28 at Meishan (Jin et al., 2000). Younger extinctions of local effect included the disappearance of a small number of "Permian-type" genera that survived into the late Griesbachian (e.g. a few Permian-type brachiopods and some tiny foraminifers) which was alternatively interpreted as a second phase of the end-Permian mass extinction at the Meishan Section (Xie et al., 2005). The top of the extinction level occurs at the top of the *Waagenites* Bed in the Selong Xishan section or possibly lowermost part of the *Otoceras* Bed (Wignall and Newton, 2003), the top of Kathwai Member A in the Salt Range sections and the top of Unit E_1 of the Khunamuh Formation in Kashmir. The upper level of the mass extinction is immediately followed by a burst of Triassic taxa such as the conodonts *Clarkina tulongensis*, *C. taylorae*, and *C. carinata* (including *planata* type forms), the ammonoids *Otoceras latilobatum*, *O. woodwardi* and *Ophiceras* spp., and the bivalve *Claraia* with extremely high abundance. Wignall and Newton (2003) claimed a late Griesbachian mass extinction at the Selong Xishan section mainly based on the last occurrences of nine foraminifer genera and calcareous sponges. Among the listed nine foraminifer genera, only *Colaniella* and *Dagmarita* have never been recorded from the Triassic before. All other foraminifers have been previously recorded from the lower Triassic (Ueno, pers. comm.). These foraminifera obviously migrated into this peri-Gondwana region following the extinction event and survived until near the end of the Griesbachian; their extinction coincided with a level that recorded a decline of benthic oxygen levels (Wignall and Newton, 2003). Wignall and Newton (2003) contrasted this Late Griesbachian dysoxic/anoxic record with the early Griesbachian record seen in many other sections including British Columbia, Canada. Given that our analysis points to a synchronous extinction event, it would appear that diachroneity is manifested only in the arrival of anoxia, which may seemingly discount anoxia as a causal mechanism contributing to the PTB event.

The last occurrences of many brachiopods and gastropods are apparently far below the PTB at the Qubu and Tulong sections in the Mt. Everest area in southern Tibet. We interpret that the earlier disappearances of many Permian benthic taxa (notably brachiopods) may be related to facies changes and possibly preservational aspects (unidentifiable small brachiopods are found 60 cm below the top of the Nimaluoshenza Member), although a somewhat more gradual or step-wise extinction prior to the rapid event cannot be ruled out. At these two sections, the topmost part of the Lopingian is composed of black silty shale and siltstone with abundant terrigenous input in a restricted inner shelf environment (Shen et al., 2003a), where large brachiopod communities would not normally be able to become firmly established (Fig. 15).

The lower level of the extinction interval is largely constrained by the sequence boundary indicated by some beds of regressive origin and the first sharp drop of both inorganic and organic carbon isotope excursions above the sequence boundary, but below the PTB; the isotopic excursions seem to be independent of lithology. This level occurs at the top of the Selong Group (Caliche Bed) at the Selong Xishan section (Jin et al., 1996 and this paper), about 20 cm below the dolostone unit at the Qubu section, the top of the White Sandstone Unit at the Salt Range section and the basal Khunamuh Formation in Kashmir (Baud et al., 1996; Brookfield et al., 2003). Below this lower extinction level, Permian taxa are abundant (Fig. 15).

The marine faunal shift recorded in the peri-Gondwanan region is basically comparable in timing to other well-studied sections such as the Meishan Section in South China (Bowring et al., 1998; Jin et al., 2000), Kapp Starostin of Spitsbergen (Wignall and Twitchett, 1996) and Jameson Land of East Greenland (Twitchett et al., 2001). According to Jin et al. (2000), a rapid extinction occurred at Bed 25 of the Meishan Section D followed by a gradual decline of a few surviving taxa until Bed 34. The major end-Permian sequence boundary is at the top of Bed 24d (Yin et al., 1996). A 2.3‰ sharp drop of $\delta^{13}C_{carb}$ occurred within the topmost 1 cm of Bed 24e (Cao et al., 2002), which are both correlatable with those of the sections in the peri-Gondwanan margin. This indicates that the Late Permian extinction event is not diachronous as Wignall and Newton (2003) suggested, but rather that it is synchronous on a global basis. However, the magnitude of extinctions associated with this event differs because of variations in biotic signature in older Permian intervals; few organisms make it to the event interval at Tulong, for example.

The strata representing this extinction interval vary in thickness. At the Selong Xishan section this interval is only about 6–17 cm, which is very similar to the Meishan section probably due to high condensation near the PTB (Shen and Jin, 1999). At the Qubu and Tulong sections, the same interval is more than 1 m in thickness although the resolution of the event is low because of facies and preservational problems. Although the stratigraphic ranges of various fossils in the five sections show a stepwise accelerating decline close to the PTB (see Figs. 4, 10, 12 and 13), we consider the extinction pattern to be very rapid. The stratigraphic stepwise patterns are probably due to backward smearing of the last occurrences because of the well-known "Signor-Lipps Effect".

6.2. Rapid change from cooling to warming climate during Late Changhsingian

The peri-Gondwanan sections reviewed here were situated in the southern mesothermal temperate zone, within the broad biogeographical transitional zone between the Gondwanan and Palaeoequatorial realms (Shi et al., 1995). As such they are more likely to record sensitive information regarding climatic changes as expressed by changes in faunal successions. Warm-water forms may invade southward with the climatic warming; conversely cold-water forms would migrate northward if the climate becomes cooler.

The climate prior to the end-Permian mass extinction in the peri-Gondwanan margin was cold. However, a climatic warming event was indicated by the faunal changes just beneath the PTB. At the Selong Xishan section, the climate prior to the Coral Bed was cold as indicated by typical Gondwanan cold-water brachiopods such as *Taeniothaerus*, *Trigonotreta* and large thick-shelled *Spiriferella*, *Neospirifer*, etc., and the absence of conodonts. Climatic warming during the Permian-Triassic transition is indicated by the occurrence of abundant conodonts. Although some conodont species (e.g. *Mesogondolella sheni*) are cold-water types (Mei and Henderson, 2001), many other species are suggestive of warm-water conditions (*Clarkina* spp.). Furthermore, it is significant to note that conodonts become abundant in the uppermost parts of the Selong Group and the overlying Kangshare Formation after a considerable barren interval in the lower and middle parts of the Selong Group. This sudden invasion is almost certainly indicative of a climatic warming event. Wignall and Newton (2003) also pointed to calcareous sponges as Tethyan immigrants into this peri-Gondwanan section. A comparable pattern has been recognised in the Canadian Arctic (Henderson and Baud, 1997) with the immigration of warm-water conodonts. This interpretation is also supported by the change of brachiopod composition from the Selong Group to the basal Kangshare Formation (the *Waagenites* Bed). The brachiopods in the basal Kangshare Formation are characterised by some small thin-shelled brachiopods associated with some warm-water and cosmopolitan elements (Fig. 3). *Tethyochonetes*, which is very common in the Palaeoequatorial Cathaysian Province during the Changhsingian (Lopingian) and P–T transition, and many other widely-distributed elements (e.g. *Girtyella*, *Hustedia*, *Martinia*) in the Palaeoequatorial Realm, invaded the Himalayan Zone in the *Waagenites* Bed (Fig. 3A). The presence of the Caliche Bed at the Selong Xishan section indicates a semi-arid, warm climatic setting, which is also consistent with implications from the biotic changes.

At the Qubu section, conodonts are totally absent in the lower member of the Qubuerga Formation. The same conodont assemblage as that at the Selong Xishan section began to occur in the basal dolostone unit of the Tulong Formation. Although small brachiopods commonly present in the PTB beds have not been found from the micaceous shale and the overlying dolostone unit of the Tulong Formation, a gastropod assemblage dominated by *Bellerophon*, *Naticopsis* and *Retispira* is present in the black micaceous shale and siltstone of the upper Nimaluoshenza Member of the Qubuerga Formation. This gastropod assemblage has been widely recorded in North America, Malaysia and South China, and therefore probably also implies the southern invasion of warm-water benthic faunas (Pan et al., in preparation).

In the Salt Range, Pakistan, conodonts in the Chhidru Formation are characterised by typical cold-water elements such as *Vjalovognathus* and *Merrillina* followed by the warm-water *Clarkina meishanensis* Zone in the basal Kathwai Member. Brachiopods in the Kalabagh Member of the Upper Wargal Formation exhibit an admixture between the warm-water Tethyan species and the cold-water Gondwanan species. However, brachiopods in the basal Kathwai Member (Grant, 1970) are dominated by warm-water Tethyan types such as *Spinomarginifera*, *Ombonia*, *Orthothetina* and *Enteletes*, which have never been found in bipolar regions. In Kashmir, the brachiopods and bivalves in Unit E_1 of the Khunamuh Formation are also dominated by the Tethys-type forms such as *Orthothetina*, *Araxathyris* and *Etheripecten* (Shimizu, 1981).

The climatic change from cooling to warming during the Late Permian in Gondwana is also reflected in the Permian-Triassic sequence of the Canning Basin in Western Australia and eastern Australia (Veevers et al., 1994; Retallack, 1999). The Lopingian Hardman Formation in the Canning Basin is characterised by typical cold-water brachiopods (Archbold, 1988) and conodonts (Nicoll and Metcalfe, 1998). Recently, two brachiopod assemblages were recognised from the latest Permian in a borehole (Thomas et al., 2004). The lower assemblage includes the brachiopods *Marginifera* and *Auritusinia*, which imply a cold-water affinity. In contrast, the upper assemblage contains the productid *Spinomarginifera* sp. (Thomas et al., 2004), which is very common in the Lopingian of South China. In the Sydney Basin of eastern Australia, the Late Permian *Glossopteris*- and dropstone-bearing coal measures were replaced by the *Dicroidium*-bearing sediments with redbeds, but without coal, therefore also indicating a transfer from a cold

climate to warm climate (Veevers et al., 1994). This is supported by the study on the palaeosol across the PTB in the Sydney Basin (Retallack, 1999).

It is significant that the climatic change from cooling to warming in the southern hemisphere was also documented from the northern hemisphere (Beauchamp, 1994; Beauchamp and Baud, 2002; Chumakov and Zharkov, 2003). The biotic succession of the Sverdrup Basin, Canadian Arctic records a significant cooling condition from the Kungurian and especially during the latest Permian as indicated by a siliceous sponge-dominated biota (hyalosponge) in shallow-water chert (Beauchamp, 1994). The chert suggests environmental conditions similar to those prevailing on modern polar shelves. Hyalosponge chert units indicating similar cooling trends also exist from northern Alaska to the Timan-Petchora Basin (Stemmerik and Worsley, 1989). By the latest Changhsingian (Henderson and Baud, 1997; Henderson and Mei, 2000), the chert-rich van Hauen Formation is overlain by the chert-free Blind Fiord Formation in the Sverdrup Basin, which is interpreted to have resulted from latest Permian warming (Beauchamp and Baud, 2002). Evidence for global warming is also indicated by the cessation of glaciation in polar areas and migration of thermophilic flora toward high latitudes (Chumakov and Zharkov, 2003).

In summary, a climatic warming event near the very end of the Permian in the peri-Gondwanan region is indicated (Fig. 15). Initially, this warming event resulted in the migration of several new warm-water, Permian-type taxa into the peri-Gondwana region and a change, if not increase, in taxonomic diversity. Ultimately, this rapid warming event may have been a contributing factor toward the subsequent Late Permian extinction event. Climatic warming probably resulted from widespread volcanic activity or by release of methane from clathrates during the latest Permian, both of which could have caused rapid warming by the greenhouse effect. The release of methane from clathrate hydrates beneath the sea floor has been an appealing causal mechanism of late because it could also have caused the negative carbon isotopic shift. However, Payne et al. (2004) largely discount this possibility by demonstrating even larger negative shifts later in the Triassic including the Early Olenekian, less than 2 million years later, providing insufficient time to replenish methane reservoirs; they cannot all be associated with methane release. Furthermore, the main warming event is coincident with transgression, which normally would not have led to methane release, as the release of pressure from retreating seas would appear to be necessary to produce this effect. In contrast, the flood basalts in Siberia and many tuffaceous or ash beds near the PTB in South China have provided evidence indicating possible temporal and causal links with the end-Permian mass extinction (Campbell et al., 1992; Renne et al., 1995; Bowring et al., 1998) and may have been an important factor for warming by venting CO_2.

6.3. Rapid transgression during latest Changhsingian following a major Late Permian regression

Sequence terminology is based on the T–R sequence concept of Embry and Johannessen (1992) and Embry (1995); they defined a sequence boundary at the subaerial unconformity or at the correlative conformity defined by the maximum regressive surface. As such, a sequence is subdivided into regressive and transgressive systems tracts. The upper regressive system tract (Fig. 15) more or less coincides with late highstand and/or lowstand systems tracts of other authors (e.g. Posamentier et al., 1988).

A sequence boundary indicated by a regressive event can be recognised from the above five sections in the peri-Gondwanan region (Fig. 15). This sequence boundary is in the Caliche Bed at the Selong Xishan section, the micaceous shale and siltstone member at the Qubu and the Tulong sections, the White Sandstone Unit in the Salt Range, Pakistan and the top of the Zewan Formation in Kashmir. It can be correlated with the Late Changhsingian sequence boundary at the top of Bed 24d at Meishan, South China. Above the sequence boundary, fining upward lithofacies changes are recorded across the PTB. The PTB sequences of the five sections in the peri-Gondwanan region show a rapid biofacies change from benthic to nektic taxa-dominated communities. Pyritic horizons have been detected near the PTB at the Selong Xishan and Qubu sections (Figs. 6G and 9G,H). This evidence indicates a rapid transgression beginning during the latest Changhsingian in the peri-Gondwanan region. This deepening is also indicated by the sudden influx of gondolellid taxa, usually above the sequence boundary (Lai et al., 2001). This transgressive event is comparable with that recorded at the Meishan section in South China and many other regions in the world (Hallam and Wignall, 1999). This rapid transgression may have also resulted from the widespread greenhouse effect during the end-Changhsingian or by tectonic effects at least in part associated with Siberian trap volcanism.

7. Conclusions

Detailed palaeontology and carbon-isotope chemostratigraphy in the peri-Gondwanan region provide the

needed framework to better interpret the Late Permian extinction in higher south latitudes and to make comparisons globally, including with the stratotype PTB interval at Meishan, South China. The peri-Gondwanan extinction is concentrated within a relatively narrow interval during the latest Changhsingian and possibly earliest Triassic and is synchronous with an event of similar magnitude and timing as at Meishan; it is not diachronous as previously suggested. The peri-Gondwanan Late Permian extinction interval largely coincides with a transgressive succession accompanied by major warming as indicated by biotic migration and turnover. This warming event is also recorded in many Tethyan localities and higher north latitude Arctic sections pointing to a global signature. The actual cause of this global warming event and its relationship with a major transgression remains equivocal, but Siberian trap volcanism is a leading candidate. Regardless of the ultimate cause, apparently a series of global endogenic factors must have been a major component leading to relatively rapid catastrophic dynamics and a globally synchronous tipping point that resulted in Earth's Greatest Extinction.

Acknowledgements

We are grateful to Yu-Gan Jin (Nanjing, China) for providing many constructive suggestions on various aspects of the work and Douglas H. Erwin (Washington, DC, USA) and Paul B. Wignall (Leeds, UK) for very helpful review and comments. Katsumi Ueno (Fukuoka, Japan) helped in the identification of foraminifers. Hua-Zhang Pan (Nanjing, China) identified the gastropods. Zong-Jie Fang (Nanjing, China) identified the bivalves. Yuri Zakharov (Vladivostok, Russia) identified the Triassic ammonoids of the Qubu section. Li-Chang Lu (Nanjing, China) studied the palynomorphs of the Qubu Section. Shi-Long Mei (Edmonton, Canada) gave a preliminary identification for the conodonts of the Qubu and Selong Xishan sections. Bob Nicoll (Canberra, Australia) provided some discussions on species of the conodont genus *Hindeodus*. Conodonts from the topmost part of the Coral Bed at the Selong Xishan section were provided by Feng-Sheng Xia (Nanjing, China). Yao-Song Xue (Nanjing, China), Chuan-Ming Zhou (Nanjing, China) and Zhuang-Fu Li (Xuzhou, China) are thanked for their help in the lithological studies. The photo of the Tulong section in Fig. 2E is provided by Jin Xiaochi of Chinese Academy of Geological Sciences. This study is supported by NSFC Grant (nos. 40225005 and 40321202) and the Major Basic Research Project (G200077700) of MST of China as well as an Australian Research Council grant and NSFC Grant (no. 40328003) to GRS. The contributions of Charles M. Henderson were supported by a NSERC Discovery Grant from Canada.

References

Archbold, N.W., 1988. Studies on Western Australian Permian brachiopods 8. The Late Permian brachiopod fauna of the Kirkby Range Member, Canning Basin. Proc. Royal Soc. Vic. 100, 21–32.

Baud, A., Margaritz, M., Holser, W.T., 1989. Permian-Triassic of the Tethys: carbon isotope studies. Geologische Rundschau 78 (2), 649–677.

Baud, A., Atudorei, V., Sharp, Z., 1996. Late Permian and early Triassic evolution of the northern Indian margin: carbon isotope sequence stratigraphy. Geodianam. Acta 9, 57–77.

Beauchamp, B., 1994. Permian climatic cooling in the Canadian Arctic. In: Klein, G.D. (Ed.), Pangea: Paleoclimate, tectonics, and sedimentation, zenith, and breakup of a supercontinent, vol. 288. Geolog. Soc. Am., pp. 229–246 (special paper).

Beauchamp, B., Baud, A., 2002. Growth and demise of Permian biogenic chert along northwest Pangea: evidence for end-Permian collapse of thermohaline circulation. Palaeogeogr., Palaeoclimatol., Palaeoecol. 184, 37–63.

Becker, L., Poreda, R.J., Hunt, A.G., Bunch, T.E., Rampino, M., 2001. Impact event at the Permian-Triassic boundary: evidence from extraterrestrial noble gases in Fullerenes. Science 291, 1530–1533.

Becker, L., Poreda, R.J., Basu, A.R., Pope, K.O., Harrison, T.M., Nicholson, C., Lasky, R., 2004. Bedout: a possible end-Permian impact crater offshore of northwestern Australia. Science 304, 1469–1476.

Bowring, S.A., Erwin, D.H., Jin, Y.G., Martin, M.W., Davidek, K., Wang, W., 1998. U/Pb zircon geochronogy and tempo of the end-Permian mass extinction. Science 280, 1039–1045.

Brookfield, M.E., Twitchett, R.J., Goodings, C., 2003. Palaeoenvironments of the Permian-Triassic transition sections in Kashmir, India. Palaeogeogr., Palaeoclimatol., Palaeoecol. 198, 353–371.

Campbell, I.H., Czamanske, G.K., Fedorenko, V.A., Hill, R.I., Stepanov, V., 1992. Synchrionism of the Siberian traps and the Permian-Triassic boundary. Science 258, 1760–1763.

Cao, C.Q., Wang, W., Jin, Y.G., 2002. Carbon isotope excursions across the Permian-Triassic boundary in the Meishan section, Zhejiang Province, China. Chin. Sci. Bull. 47, 1125–1129.

Chumakov, N.M., Zharkov, M.A., 2003. Climate during the Permian-Triassic biosphere reorganizations. Article 2. Climate of the Late Permian and Early Triassic: general inferences. Stratigr. Geolog. Correlat. 11 (4), 361–375.

Embry, A., 1995. Sequence boundaries and sequence hierarchies: problems and proposals. In: Steel, R.J., Felt, V.L., Johannessen, E.P., Mathieu, C. (Eds.), Sequence Stratigraphy on the Northwest European Margin, vol. 5. Norwegian Petroleum Society, Special Publication, pp. 1–11.

Embry, A., Johannessen, E., 1992. T-R sequence stratigraphy, facies analysis and reservoir distribution in the uppermost Triassic-Lower Jurassic succession, western Sverdrup Basin, Arctic Canada. In: Vorren, T.O. (Ed.), Arctic Geology and Petroleum Potential, vol. 2. Norwegian Petroleum Society Special Publication, pp. 121–146.

Erwin, D.H., 1993. The Great Paleozoic Crisis: Life and Death in the Permian. Columbia University Press, New York.

Erwin, D.H., Bowring, S.A., Jin, Y.G., 2002. End-Permian mass extinctions: a review. In: Koeberl, C., MacLeod, K.G. (Eds.), Catastrophic

Events and Mass Extinctions: Impacts and Beyond, vol. 356. Geological Society of America, pp. 363–383 (special paper).

Estaban, M., Klappa, C.F., 1983. Subaerial exposure environments. In: Scholle, P.A., Bebout, D.G., Moore, C.H. (Eds.), Carbonate Depositional Environments, vol. 33. American Association of Petroleum Geologists Memoir, pp. 2–54.

Grant, R.E., 1970. Brachiopods from Permian-Triassic boundary beds and age of Chhidru Formation, West Pakistan. In: Kummel, B., Teichert, C. (Eds.), Stratigraphic Boundary Problems: Permian and Triassic of West Pakistan, vol. 4. University of Kansas, Department of Geology, pp. 117–151 (special publication).

Hallam, A., Wignall, P.B., 1997. Mass Extinctions and their Aftermath. Oxford University Press, Oxford.

Hallam, A., Wignall, P.B., 1999. Mass extinctions and sea-level changes. Earth Sci. Rev. 48, 217–250.

Haq, B.U., 1987. Brief discussion of the Salt Range sections. IGCP Project 199-Field seminar on the Permian-Triassic succession in the Salt Range, Pakistan, Field Guide, pp. 1–22.

Henderson, C.M., 1997. Uppermost Permian conodonts and the Permian-Triassic boundary in the western Canada sedimentary basin. Bull. Can. Petroleum Geol. 45 (4), 693–707.

Henderson, C.M., Baud, A., 1997. Correlation of the Permian-Triassic boundary in Arctic Canada and comparison with Meishan, China. In: Wang, N.W., Remane, J. Proceedings of the 30th International Geological Congress, vol. 11, pp. 143–152.

Henderson, C.M., Mei, S.L., 2000. Preliminary cool water Permian conodont zonation in North Pangea: re review. Permophiles 36, 16–23.

Holland, S.M., 2000. The quality of the fossil record: a sequence stratigraphic perspective. In: Erwin, D.H., Wing, S.L. (Eds.), Deep Time, Paleobiology's Perspective, Supplement to 26 (4), pp. 148–168.

Holser, W.T., Schönlaub, H.P., Attrep M.Jr., Boeckelmann, K., Klein, P., Magaritz, M., Orth, C.J., Fenninger, A., Jenny, C., Kralik, M., Mauritsch, H., Pak, E., Schramm, J.M., Stattegger, K., Schmöller, P., 1989. A unique geochemical record at the Permian/Triassic boundary. Nature 337, 39–44.

Isozaki, Y., 1997. Permo-Triassic boundary superanoxia and stratified superocean: records from lost deep sea. Science 276, 235–238.

Jin, Y.G., Shen, S.Z., Zhu, Z.L., Mei, S.L., Wang, W., 1996. The Selong Xishan section, candidate of the global stratotype section and point of the Permian-Triassic boundary. In: Yin, H.F. (Ed.), The Palaeozoic-Mesozoic Boundary Candidates of the Global Stratotype Section and Point of the Permian-Triassic Boundary. China University of Geosciences Press, Wuhan, pp. 127–137.

Jin, Y.G., Wang, Y., Wang, W., Shang, Q.H., Cao, C.Q., Erwin, D.H., 2000. Pattern of marine mass extinction near the Permian-Triassic boundary in South China. Science 289, 432–436.

Kaiho, K., Kajiwara, Y., Nakano, T., Miura, Y., Kawahata, H., Tazaki, K., Ueshima, M., Chen, Z.Q., Shi, G.R., 2001. End-Permian catastrophe by a bolide impact: evidence of a gigantic release of sulfur from mantle. Geology 29, 815–818.

Kapoor, H.M., 1992. Permo-Trassic boundary of the Indian subcontinent and its intercontinental correlation. In: Sweet, W.C., Yang, Z.Y., Dickins, J.M., Yin, H.F. (Eds.), Permo-Triassic Events in the Eastern Tethys. World and Regional Geology 2. Cambridge University Press, Cambridge, pp. 21–36.

Kapoor, H.M., 1996. The Guryul Ravine section, candidate of the global stratotype and point (GSSP) of the Permian-Triassic boundary (PTB). In: Yin, H.F. (Ed.), The Paleozoic-Mesozoic Boundary. Candidates of the Global Stratotype Section and Point of the Permian-Triassic boundary. China University of Geosciences Press, Wuhan, pp. 99–110.

Krull, E.S., Retallack, G.J., 2000. $\delta^{13}C$ depth profiles from paleosols across the Permian-Triassic boundary: evidence from methane release. Bull. Geol. Soc. Am. 112, 1459–1472.

Krull, E.S., Lehrmann, J., Druke, D., Kessel, B., Yu, Y.Y., Li, R.X., 2004. Stable carbon isotope stratigraphy across the Permian-Triassic boundary in shallow marine carbonate platforms, Nanpanjiang Basin, south China. Palaoegeogr., Palaeoclimatol., Palaeoecol. 204, 297–315.

Krystyn, L., Baud, A., Richoz, S., Twitchett, R.J., 2003. A unique Permian-Triassic boundary section from Oman. Palaeogeogr., Palaeoclimatol., Palaeoecol. 191, 329–344.

Kummel, B., Teichert, C., 1970. Stratigraphy and paleontology of the Permian-Triassic boundary beds, Salt Range and Trans-Indus Range, West Pakistan. In: Kummel, B., Teichert, C. (Eds.), Stratigraphic Boundary Problems: Permian and Triassic of West Pakistan. University of Kansas, Department of Geology, vol. 4, pp. 1–110 (special publication).

Lai, X.L., Wignall, P.B., Zhang, K.X., 2001. Palaeoecology of the conodonts *Hindeodus* and *Clarkina* during the Permian-Triassic periods. Palaeogeogr., Palaeoclimatol., Palaeoecol. 171, 63–72.

Margaritz, M., Baud, A., Holser, W.T., 1988. The carbon-isotope shift at the Permian-Triassic boundary in the southern Alps is gradual. Nature 331, 337–339.

Marshall, C.R., 1995. Distinguishing between sudden and gradual extinctions in the fossil record: Predicting the position of the Cretaceous-Tertiary iridium anomaly using ammonite fossil record on Seymour Island, Antarctica. Geology 23, 731–734.

Matsuda, T., 1981. Early Triassic conodonts from Kashmir, India. Part 1: *Hindeodus* and *Isarcicella*. J. Geosci., Osaka City Univ. 24 (3), 75–108.

Matsuda, T., 1982. Early Triassic conodonts from Kashmir, India. Part 2: *Neospathodus* 1. J. Geosci., Osaka City Univ. 25 (6), 87–102.

Matsuda, T., 1983a. Early Triassic conodonts from Kashmir, India. Part 3: *Neospathodus* 2. J. Geosci., Osaka City Univ. 26 (4), 87–110.

Matsuda, T., 1983b. Early Triassic conodonts from Kashmir, India, Part 4: *Gondolella* and *Platyvillosus*. J. Geosci., Osaka City Univ. 27 (4), 119–141.

Mei, S.L., 1996. Restudy of conodonts from the Permian-Triassic boundary beds at Selong and Meishan and the natural Permian-Triassic boundary. In: Wang, H.Z., Wang, X.L. (Eds.), Centennial Memorial Volume of Prof. Sun Yunzhu: Palaeontology and Stratigraphy. China University of Geosciences Press, Wuhan, pp. 141–148.

Mei, S.L., Henderson, C.M., 2001. Evolution of Permian conodont provincialism and its significance in global correlation and paleoclimate implication. Palaeogeogr., Palaeoclimatol., Palaeoecol. 170, 237–260.

Mei, S.L., Henderson, C.M., 2002. Comments on some Permian conodont faunas reported from southeast Asia and adjacent areas and their global correlation. J. Asian Earth Sci. 20, 599–608.

Mei, S.L., Henderson, C.M., Wardlaw, B.R., Shi, X.Y., 1999. On provincialism, evolution and zonation of Permian and earliest Triassic conodonts. In: Yin, H.F., Tong, J.N. (Eds.), Proceedings of the International Conference on Pangea and the Paleozoic-Mesozoic Transition. China University of Geosciences Press, Wuhan, pp. 22–28.

Mertmann, D., 1999. Das marine Perm in der Salt Range und in den Trans Indus Ranges, Pakistan. Berliner Geowissenschaftliche Abhandlungen A 204, 1–94.

Mertmann, D., 2000. Foraminiferal assemblages in Permian carbonates of the Zaluch Group (Salt Range and Trans Indus Ranges Pakistan).

Neues Jahrbuch für Geologie und Paläontologie Monatshefte (3), 129–146.

Mertmann, D., 2003. Evolution of the marine Permian carbonate platform in the Salt Range (Pakistan). Palaeogeogr., Palaeoclimatol., Palaeoecol. 191, 373–384.

Morante, R., 1996. Permian and Early Triassic isotopic records of carbon and strontium in Australia and a scenario of events about the Permian-Triassic boundary. Historical Biol. 11, 289–310.

Mundil, R., Metcalfe, I., Ludwig, K.R., Renne, P.R., Oberli, F., Nicoll, R.S., 2001. Timing of the Permian-Triassic biotic crisis: implications from new zircon U/Pb age data (and their implications). Earth Planetary Sci. Lett. 187, 131–145.

Mundil, R., Ludwig, K.R., Metcalfe, I., Renne, P.R., 2004. Age and timing of the Permian mass extinctions: U/Pb dating of closed-system zircons. Science 305, 1760–1763.

Nakazawa, K. (Ed.), 1981. The Upper Permian and Lower Triassic faunas of Kashmir, vol. 46. Palaeontologica Indica, pp. 1–204, New Series.

Nakazawa, K., 1993. Stratigraphy of the Permian-Triassic transition and the Palaeozoic/Mesozoic boundary. Bull. Geolog. Survey Jpn. 44 (7), 425–445 (in Japanese).

Nakazawa, K., Kapoor, H.M., Ishii, K., Bando, Y., Okimura, Y., Tokuoka, T., 1975. The Upper Permian and the Lower Triassic in Kashmir, India. Memoirs Kyoto Univ., Fac. Sci. (Geol. Mineral.) 42 (1), 1–106.

Nicoll, R.S., Metcalfe, I., 1998. Early and Middle Permian conodonts from the Canning Basin and southern Cararvon Basins, western Australia: their implications for regional biogeography and palaeoclimatology. In: Shi, G.R., Archbold, N.W., Grover, M. (Eds.), The Permian System: Stratigraphy, Palaeogeography and Resources, Proceedings of the Royal Society of Victoria, vol. 110, pp. 419–461.

Orchard, M.J., Nassichuk, W.W., Rui, L., 1994. Conodonts from the lower Griesbachian *Otoceras latilobatum* Bed of Selong, Xizang and the position of the Permian-Triassic boundary. Memoir Can. Soc. Petroleum Geol. 17, 823–843.

Pakistan-Japanese Working Group (PJWG), 1985. Permian and Triassic systems in the Salt Range and Surghar Rang, Pakistan. In: Nakazawa, K., Dickins, J.M. (Eds.), The Tethys, Her Palaeogeography and Palaeobiogeography from Palaeozoic to Mesozoic. Tokai University Press, Tokyo, pp. 221–312.

Payne, J.L., Lehrmann, D.J., Wei, J., Orchard, M.J., Schrag, D.P., Knoll, A.H., 2004. Large perturbations of the carbon cycle during recovery from the End-Permian extinction. Science 305, 506–509.

Posamentier, H., Jervey, M., Vail, P., 1988. Eustatic controls on clastic deposition II – sequence and systems tract models. In: Wilgus, C.K., Hastings, B.S., Kendall, C.G.St.C., Posamentier, H.W., Ross, C.A., Van Wagoner, J.C. (Eds.), Sea Level Changes: An Integrated Approach, vol. 42. SEPM Special Publication, pp. 125–154.

Rampino, M.R., Adler, A.C., 1998. Evidence for abrupt latest Permian mass extinction of foraminifera: results of test for the Signor-Lipps effect. Geology 26, 415–418.

Rao, R.B., Zhang, Z.G., 1985. A discovery of Permo-Triassic transitional fauna in the Qomolangma Feng area: its implications for the Permo-Triassic boundary. Xizang Geol. 1, 19–31 (in Chinese, with English abstract).

Raup, D.M., 1979. Size of the Permian-Triassic bottleneck and its evolutionary implications. Science 206, 217–218.

Reeves Jr., C.C., 1970. Origin, classification, and geologic history of caliche on the southern High Plains, Texas and eastern New Mexico. J. Geol. 78, 352–362.

Renne, P.R., Zhang, Z.C., Richards, M.A., Black, M.T., Basu, A.R., 1995. Synchrony and causal relations between Permian-Triassic boundary crises and Siberian flood volcanism. Science 269, 1413–1416.

Retallack, G.J., 1999. Postapocalyptic greenhouse paleoclimate revealed by earliest Triassic paleosols in the Sydney Basin, Australia. Bull. Geol. Soc. Am. 111, 52–70.

Retallack, G.J., 2004. Comment—contrasting deep-water records from the Upper Permian and Lower Triassic of South Tibet and British Columbia: evidence for a diachronous mass extinction (Wignall and Newton, 2003). Palaios 19, 101–102.

Retallack, G.J., Smith, R.M.H., Ward, P.D., 2003. Vertebrate extinction across Permian-Triassic boundary in Karoo Basin, South Africa. Bull. Geol. Soc. Am. 115, 1113–1152.

Sarkar, A., Yoshioka, H., Ebihara, M., Naraoka, H., 2003. Geochemical and organic carbon isotope studies across the continental Permo-Triassic boundary of Raniganj Basin, eastern India. Palaeogeogr., Palaeocliamtol., Palaeoecol. 191, 1–14.

Scholle, P.A., Kinsman, D.J.J., 1974. Aragonitic and high-Mg calcite caliche from the Persian Gulf-a modern analog for the Permian of Texas and New Mexico. J. Sediment. Res. 44, 904–916.

Sepkoski Jr., J.J., 1984. A kinetic model of Phanerozoic taxonomic diversity. III. Post-Palaeozoic families and mass extinctions. Paleobiology 10 (2), 246–267.

Shen, S.Z., Jin, Y.G., 1999. Brachiopods from the Permian-Triassic beds at the Selong section, Xizang (Tibet), China. J. Asian Earth Sci. 17, 547–559.

Shen, S.Z., Cao, C.Q., 2002. Faunal shift across the Permian-Triassic boundary in southern Tibet. NAPC 2001 Program and abstracts. PaleoBios 21 (Suppl. 2), 115–116.

Shen, S.Z., Shi, G.R., 2002. Paleobiogeographical extinction patterns of Permian brachiopods in the Asian-western Pacific Region. Paleobiology 28 (4), 449–463.

Shen, S.Z., Archbold, N.W., Shi, G.R., Chen, Z.Q., 2000. Permian brachiopods from the Selong Xishan section, Xizang (Tibet), China. Part 1: Stratigraphy, Strophomenida, Productida and Rhynchonellida. Geobios 33, 725–752.

Shen, S.Z., Archbold, N.W., Shi, G.R., Chen, Z.Q., 2001. Permian brachiopods from the Selong Xishan section, Xizang (Tibet), China. Part 2: Palaeobiogeographical and palaeoecological implications, Spiriferida, Athyridida and Terebratulida. Geobios 34, 157–182.

Shen, S.Z., Cao, C.Q., Shi, G.R., Wang, X.D., Mei, S.L., 2003a. Lopingian (Late Permian) stratigraphy, sedimentation and palaeobiogeography in southern Tibet. Newslett. Stratigr. 39 (2/3), 157–179.

Shen, S.Z., Shi, G.R., Archbold, N.W., 2003b. Lopingian (Late Permian) brachiopods from the Qubuerga Formation at the Qubu section in the Mt. Qomolangma region, southern Tibet (Xizang), China. Palaeontographica A 268, 49–101.

Shi, G.R., Shen, S.Z., 1997. A Late Permian Brachiopod Fauna from Selong, Southern Xizang (Tibet), China. Proc. Royal Soc. Vic. 109 (1), 37–56.

Shi, G.R., Archbold, N.W., Zhan, L.P., 1995. Distribution and characteristics of mid-Permian (Late Artinskian-Ufimian) mixed/transitional marine faunas in the Asian region and their palaeogeographical implications. Palaeogeogr., Palaeoclimatol., Palaeoecol. 114, 241–271.

Shimizu, D., 1981. Upper Permian brachiopod fossils from Guryul Ravine and its spur three kilometers of Barus. Palaeontol. Indica 46, 67–85, New Series.

Signor, P.W., Lipps, J.H., 1982. Sampling bias, gradual extinction patterns and catastrophes in the fossil record. In: Silver, L.T., Schultz, P.H. (Eds.), Geological Implications of Impacts of Large Asteroid

and Comets on the Earth, vol. 190. Geological Society of America, pp. 291–296 (special paper).

Smith, R.M.H., Ward, P.D., 2001. Pattern of vertebrate extinctions across an event bed at the Permian-Triassic boundary in the Karoo Basin of South Africa. Geology 29, 1147–1150.

Stemmerik, L., Worsley, D., 1989. Late Palaeozoic sequence correlation, North Greenland, Svalbard and the Barents Shelf. In: Collinson, J.D. (Ed.), Correlation in Hydrocarbon Exploration. Graham and Trotman, Norwegian Petroleum Society, London, pp. 99–111.

Sweet, W.C., 1970. Uppermost Permian and Lower Triassic conodonts of the Salt Range and Trans-Indus Ranges, West Pakistan. In: Kummel, B., Teichert, C. (Eds.), Stratigraphic Boundary Problems: Permian and Triassic of West Pakistan, vol. 4. University of Kansas, Department of Geology, pp. 207–276 (special publication).

Sweet, W.C., 1992. A conodont-based high-resolution biostratigraphy for the Permo-Triassic boundary interval. In: Sweet, W.C., Yang, Z.Y., Dickins, J.M., Yin, H.F. (Eds.), Permo-Triassic Events in the Eastern Tethys. World and Regional Geology 2. Cambridge University Press, Cambridge, pp. 120–133.

Tian, C.R., 1982. Triassic conodonts in the Tulong section from Nyalam County, Xizang (Tibet), China. Contrib. Geol. Qinghai-Xizang (Tibet) Plateau 8, 153–165 (in Chinese, with English abstract).

Thomas, B.M., Willink, R.J., Grice, K., Twitchett, R.J., Purcell, R.R., Archbold, N.W., George, A.D., Tye, S., Alexander, R., Foster, C.B., Barber, C.J., 2004. Unique marine Permian-Triassic boundary section from Western Australia. Aust. J. Earth Sci. 51, 423–430.

Twitchett, R.J., Looy, C.V., Morante, R., Visscher, H., Wignall, P.B., 2001. Rapid and synchronous collapse of marine and terrestrial ecosystem during the end-Permian biotic crisis. Geology 29, 351–354.

Twitchett, R.J., Krystyn, L., Baud, A., Wheeley, J.R., Ricjoz, S., 2004. Rapid marine recovery after the end-Permian mass-extinction event in the absence of marine anoxia. Geology 32, 805–808.

Veevers, J.J., Conaghan, P.J., Shaw, S.E., 1994. Turning point in Pangean environmental history at the Permian/Triassic (P/Tr) boundary. Geol. Soc. Am. 288, 187–196 (special paper).

Walls, R.A., Harris, W.B., Nunan, W.E., 1975. Calcareous crust (caliche) profiles and early subaerial exposure of Carboniferous carbonates, northeastern Kentucky. Sedimentology 22, 417–440.

Wang, K., Geldsetzer, H.H.J., Krouse, H.R., 1994. Permian-Triassic extinction: organic $\delta^{13}C$ evidence from British Columbia, Canada. Geology 22, 580–584.

Wang, Y.G., Chen, C.Z., Rui, L., Wang, Z.H., Liao, Z.T., He, J.W., 1989. A potential global stratotype of Permian-Triassic boundary. In: Chinese Academy of Sciences, developments in Geosciences. Contribution to 28th International Geological Congress, 1989, Washington, DC, USA. Science Press, Beijing, pp. 221–229.

Wang, Z.H., Wang, Y.G., 1995. Permian-Lower Triassic conodonts from Selong Xishan of Nyalam, S. Tibet, China. Acta Micropalaeontol. Sinica 12, 333–348.

Wardlaw, B.R., Mei, S.L., 1999. Refined conodont biostratigraphy of the Permian and lowest Triassic of the Salt and Khizor Ranges, Pakistan. In: Yin, H.F., Tong, J.N. (Eds.), Proceedings of the International Conference on Pangea and the Paleozoic-Mesozoic Transition. China University of Geosciences Press, Wuhan, pp. 154–156.

Waterhouse, J.B., Gupta, V.J., 1983. An early Djhulfian (Permian) brachiopod faunule from Upper Shyok Valley, Karakorum Range and the implications for dating of allied faunas from Iran and Pakistan. Contrib. Himalayan Geol. 2, 188–233.

Wignall, P.B., Hallam, A., 1992. Anoxia as a cause of the Permian/Triassic mass extinction: facies evidence from northern Italy and the western United States. Palaeogeogr., Palaeoclimatol., Palaeoecol. 93, 21–46.

Wignall, P.B., Hallam, A., 1993. Griesbachian (Earliest Triassic) palaeoenvironmental changes in the Salt Range, Pakistan and southeast China and their bearing on the Permo-Triassic mass extinction. Palaeogeogr., Palaeoclimatol., Palaeoecol. 102, 215–237.

Wignall, P.B., Twitchett, R.J., 1996. Oceanic anoxia and the end-Permian mass extinction. Science 272, 1155–1158.

Wignall, P.B., Newton, R., 2003. Contrasting deep-water records from the Upper Permian and Lower Triassic of south Tibet and British Columbia: evidence for a diachronous mass extinction. Palaios 18, 153–167.

Wignall, P.B., Morante, R., Newton, R., 1998. The Permo-Triassic transition in Spitsbergen: $\delta^{13}C_{org}$ chemostratigraphy, Fe and S geochemistry, facies, fauna and trace fossils. Geol. Magazine 135, 47–62.

Xia, F.S., Zhang, B.G., 1992. Age of the Selong formation in Xishan, Selong of Xizang (Tibet) and the Permian-Triassic boundary. J. Stratigr. 16, 256–363 (in Chinese, with English abstract).

Xie, S.C., Pancost, R.D., Yin, H.F., Wang, H.M., Evershed, R.P., 2005. Two episodes of microbial change coupled with Permo/Triassic faunal mass extinction. Nature 434, 494–497.

Yao, J.X., Li, Z.S., 1987. Permian-Triassic conodont faunas and the Permian-Triassic boundary at the Selong Section in Nyalam County, Xizang, China. Chin. Sci. Bull. 1, 45–51 (in Chinese, with English abstract).

Yin, H.F., Wu, S.B., Ding, M.H., Zhang, K.X., Tong, J.N., Yang, F.Q., Lai, X.L., 1996. The Meishan section, candidate of the global stratotype section and point of the Permian-Triassic boundary. In: Yin, H.F. (Ed.), The Palaeozoic-Mesozoic Boundary Candidates of the Global Stratotype Section and Point of the Permian-Triassic Boundary. China University of Geosciences Press, Wuhan, pp. 31–48.

Yin, J.X., Guo, S.Z., 1979. Stratigraphy of the Mt Jolmolangma and its northern slope, with a discussion about correlation of Sinian-Cambrian and Carboniferous-Permian with adjacent areas. In: Xizang Scientific Expedition Team of Chinese Academy of Sciences (Ed.), A Report of the Scientific Expedition in The Mt. Jolmolangma Region (1975) (Geology). Science Press, Beijing, pp. 1–71 (in Chinese).

Ziegler, A.M., Hulver, M.L., Roeley, D.B., 1997. Permian world topography and climate. In: Martini, I.P. (Ed.), Late Glacial and Postglacial Environmental Changes-Quaternary, Carboniferous-Permian and Proterozoic. Oxford University Press, New York, pp. 111–146.